

**Critical Gradient for Internal Erosion in Earthen Dams:  
A Comparative Analysis of Two Predictive Methodologies**

by

Catherine Donohue  
B.S. Civil Engineering  
Lehigh University, Bethlehem, PA

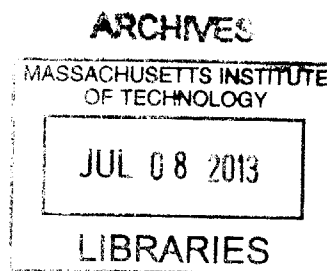
Submitted to the Department of Civil and Environmental Engineering in partial fulfillment of the requirements for the degree of

Master of Engineering in Civil and Environmental Engineering

at the

MASSACHUSETTS INSTITUTE OF TECHNOLOGY  
June 2013

© 2013 Catherine Donohue. All rights reserved



The author hereby grants to MIT permission to reproduce and to distribute publicly paper and electronic copies of this thesis document in whole or in part in any medium now known or hereafter created.

Signature of Author.....  
Department of Civil and Environmental Engineering  
May 24, 2013

Certified by.....  
Herbert H. Einstein  
Professor of Civil and Environmental Engineering  
Thesis Supervisor

Accepted by.....  
Heidi M. Nepf,  
Chair, Departmental Committee for Graduate Students



**Critical Gradient for Internal Erosion in Earthen Dams:  
A Comparative Analysis of Two Predictive Methodologies**

by

Catherine Donohue

Submitted to the Department of Civil and Environmental Engineering  
on May 24, 2013, in partial fulfillment of the requirements for the degree of  
Master of Engineering in Civil and Environmental Engineering

**ABSTRACT**

Minimizing the uncertainty in predicting the critical gradient of a dam (i.e. the critical reservoir pool level) is important during the risk analysis of dams. Uncertainty leads to inexact relative risk in portfolio management; therefore it is essential to get as accurate a risk estimation as possible for each project in a portfolio. To understand the uncertainty inherent in the predictive methodologies, this thesis sets out to compare the two most commonly used predictive methodologies, Sellmeijer and Schmertmann, in the USACE portfolio in order to make a suggestion of when to use which. Both methodologies have been calibrated for a small range of ideal soil characteristics that may not reflect of existing conditions of the portfolio. This thesis concludes with the recommendation to broaden the range of applicability through additional experiments that include anisotropic conditions.

Thesis Supervisor: Herbert H. Einstein  
Title: Professor of Civil and Environmental Engineering

## **ACKNOWLEDGEMENTS**

I am so grateful to Professor Einstein for the hours he invested in this thesis.

Professor Einstein is an extraordinary educator, and the heart and soul of the Geotech department. I am blessed that Professor Einstein agreed to advise me, and am honored to call myself his student.

I would like to thank Dr. Jen for teaching me a “girl’s guide to soil mechanics”. I proudly report to her that my OCR is now greater than one.

I am indebted to Pamela and Thalia of the MIT Writing Center. This thesis would have been more arduous and stressful without their expert advice.

John, Eric, Tammy, and Nate, thank you for sharing my vision.

And to my sister Tricia - you have been my buddy since the beginning, and provide the safety line every time I push my boundaries. Thank you for supporting my many crazy pursuits. I am going off belay; until the next adventure...

# Table of Contents

ABSTRACT.....	3
ACKNOWLEDGEMENTS.....	4
1.0 Introduction .....	9
1.1 Statistics on US Dam Failure Modes .....	13
1.2 Seepage and Piping.....	13
2.0 Background .....	19
2.1 Enterprise Risk Management.....	20
2.2 Infrastructure Investment Challenges .....	21
2.3 Portfolio Risk Management .....	23
2.4 Tolerable Risk.....	23
2.5 Failure Mode, Effects, and Criticality Analysis .....	25
2.4.1 Event Tree Analysis .....	29
3.0 Methods for Determining the Critical Gradient of a Dam .....	33
3.1 Bligh.....	34
3.2 Terzaghi.....	35
3.3 Lane .....	37
3.4 Sellmeijer .....	39
3.5 Schmertmann.....	46
3.6 Processing Case Study Data .....	51
4.0 Parameters and Data Analysis .....	53
4.1 Case Studies .....	54
4.2 Input Parameters .....	58
4.3 Results and Discussion .....	64
4.3.1 Case Study Results with Idealized Soil Conditions .....	65
4.3.2 Case A Results.....	67
4.3.3 Case B Results.....	68

5.0 Conclusions and Recommendations .....	73
5.1 Recommendations for Using Sellmeijer and Schmertmann Methodologies.....	75
5.2 Recommendations for Future Study.....	77
References .....	79
Websites consulted.....	81
Appendix A.....	82
Appendix B.....	85
Appendix C.....	88
Appendix D.....	91
Appendix F.....	97
Appendix G.....	100

# Table of Figures

Figure 1.1 National Performance of Dams.....	13
Figure 1.2 Sketch of Hydraulic Gradient and Potential Pipe Path .....	14
Figure 1.3 Illustration of the Onset of Seepage .....	15
Figure 1.4 Illustration of the Onset of Piping.....	16
Figure 1.5 Illustration of the Behavior of a Pipe Channel Progression in a Model Simulation.....	17
Figure 2.1 Generic Enterprise Risk Management Process .....	21
Figure 2.2 Risk Effects in a Floodplain.....	22
Figure 2.3 USACE Tolerable Risk Guideline.....	24
Figure 2.4 Relative Plotting Position of 25 Sample Projects .....	25
Figure 2.5 Effect of Adjusting the Probabilities of Potential Failure Modes.....	27
Figure 2.6 Monte Carlo Simulation Determining the Probability of a Potential Failure Mode .....	28
Figure 2.7 Internal Erosion Potential Failure Mode Sub-event Tree .....	30
Figure 3.1 Flow Path of an Idealized Water Molecule under the Dam.....	37
Figure 3.2 Subset of Lane Data for Sand, Fine Sand, and Silt .....	39
Figure 3.3 Visual Representation of the Parameters Used in Sellmeijer Methodology .....	41
Figure 3.4 Two Force Balance of a Top Grain .....	42
Figure 3.5 Schmertmann Correlation for Determining $i_{pmt}$ .....	49
Figure 3.6 Adjustment to the Schmertmann Correlation for Determining $i_{pmt}$ .....	50
Figure 4.1 Case A Dam Cross Section with Foundation Soil Characteristics Included .....	55
Figure 4.2 Case B Dam Cross Section with Foundation Soil Characteristics Included .....	56
Figure 4.3 Effect of Relative Density on the Sellmeijer and Schmertmann Predictive Methodology .....	62
Figure 4.4 Sellmeijer Effect of Intrinsic Permeability ( $k$ ) and Schmertmann Effect of $k_h/k_v$ .....	63
Figure 4.5 Effect of Grain Size (both $d_{10}$ and $d_{70}$ ) on the Critical Hydraulic Gradient .....	64
Figure 4.6 Case A – Results of Idealized Predicted Critical Reservoir Elevations for Each Methodology...	66
Figure 4.7 Case B – Results of Idealized Predicted Critical Reservoir Elevations for Each Methodology...	66
Figure 4.8 Case A – Predicted Critical Reservoir Elevations for Each Methodology.....	68
Figure 4.9 Case B – Predicted Critical Reservoir Elevations for Each Methodology .....	70

## List of Tables

Table 1 Comparison of Weighted Creep Ratios .....	38
Table 2 Sellmeijer Methodology Input Parameters.....	41
Table 3 Additional Sellmeijer Methodology Input Parameters .....	44
Table 4 Schmertmann Methodology Input Parameters .....	48
Table 5 Method for Obtaining the Sellmeijer Methodology Inputs .....	58
Table 6 Method for Obtaining the Schmertmann Methodology Inputs.....	59
Table 7 Case A Results of the Alluvial Layer.....	67
Table 8 Case A Results for the Glacial Layer .....	68
Table 9 Case B Results for the Alluvial Layer .....	69
Table 10 Case B Results for the Glacial Layer .....	69



## 1.0 Introduction

Large water resource projects in the United States (US), such as dams and levees, are authorized and funded by the US Congress. The 74<sup>th</sup> US Congress passed the first of many laws called Flood Control Acts in 1936. The Flood Control Act was part of the profusion of legislation meant to stimulate the economy after the Great Depression. The 1936 Flood Control Act gave the US Army Corps of Engineers (USACE) the mission to provide flood protection throughout the United States in perpetuity or until Congress deauthorizes the mission. Flood control projects are water impoundment structures, such as dams and levees, built to adjust the conveyance of water.

The American Society of Civil Engineers (ASCE) has been assessing the nation's infrastructure, and alerting Congress to the infrastructure crisis in America via a report card since 1988 (ASCE, 2013). The ASCE, a not for profit engineering association, generates an annual report card, which is used to brief Congress on the general state of the nation's critical infrastructure with 16 infrastructure categories graded. The ASCE held a summit in 2009 inviting civil engineers across the US to discuss and evaluate the infrastructure status. An outcome of this summit was the *Guiding Principles for the Nation's Critical Infrastructure* in 2009. One of the four guiding principles highlighted in this document is to "quantify, communicate and manage risk". Quantifying risk can be very challenging when uncertainty is inherent in predicting the probabilities that infrastructure will fail under different conditions and mechanisms.

Risk assessments are the device used to quantify risk. This thesis will concentrate on one critical infrastructure category, dams, within one organization, USACE, in order to understand the risk assessment process by evaluating one specific potential failure mode of the risk

assessment. This thesis focuses on the example of internal erosion as the potential failure mode in the risk assessment to understand the effect that a conservative estimate of critical gradient may have on the portfolio risk management process.

At present, there is a critical infrastructure crisis in the US (ASCE 2013). The US infrastructure is currently approaching or exceeding its expected useful service life; a typical useful service life for large water resource projects is approximately 50 years (ASCE 2013). Due to the political and economic pressures of the late 1930s, many dams were authorized and then constructed throughout the 1940s and 1950s in response to the large storm events that occurred during the 1930s. The federal dam safety projects, which protect public life and property, were built under a cost shared agreement with the local government and are a shared liability and responsibility managed by a complex partnership between the Army Corps and local governmental agencies.

The USACE has spent the last 6 years developing and implementing an extensive enterprise risk management program. The program uses a portfolio risk management process, evaluating the flood risk management project portfolio due to the mounting crisis of aging water resource projects beyond useful life expectancies ([usace.army.mil](http://usace.army.mil)). The flood risk management projects have been inventoried and assessed by the Corps. The assessments are a foundational element in the portfolio risk management process that has enabled the Army Corps to prioritize infrastructure needs and requirements. The priority queue for major rehabilitation of dams is managed at the national level and the projects are implemented at the local level. The agency is deliberately and efficiently expending limited federal funds on the highest risk projects first.

In the portfolio risk management process, a risk assessment is performed on each project in the USACE portfolio in order to quantify the condition and risk of the structure. The assessments are performed with different levels of complexity depending on the risk and the major effects of

the risk. Risk assessments evaluate condition of assets, probability of an event causing failure, and the consequences if a failure event occurs. The probability of infrastructure integrity is studied through a failure mode, effect, and criticality analysis (FMECA) by geotechnical engineers with risk subject matter experts and the consequences of infrastructure failing are independently evaluated by hydraulic engineers along with consequence subject matter experts via sophisticated hydrodynamic modeling. (Chapter 2 will provide a more detailed discussion on enterprise risk management (ERM) and failure modes, effects, and criticality analysis (FMECA)). Risk can be measured by the product of the probability of infrastructure failure and the consequences of the infrastructure failing. Understanding risk enables the USACE leadership to make risk informed prioritization decisions, and enables the local USACE offices to communicate the risk effectively to the local communities. This knowledge of the specific project risk empowers the communities to take appropriate risk reduction actions.

There are numerous typical potential failure modes for aging water impoundment infrastructure (ie, overtopping, spillway failure, internal erosion, etc.). These failure modes are identified in the FMECA study, which the Army Corps calls the potential failure mode analysis (PFMA). The most probable failure modes are analyzed independently of one another. The most uncertain failure mode is internal erosion. Due to uncertainty this failure mode is almost always analyzed in depth. Subject matter experts use event tree analysis to elicit the scenarios of failure to reduce uncertainty in the probability estimates. Potential failure mode analysis and event tree analysis will be discussed further in section 2.4.

This thesis will specifically evaluate two methodologies, developed by Sellmeijer and Schmertmann, for predicting the probability of internal erosion caused by the seepage and

pipng mechanism; in particular the critical gradient ( $i_{cr}$ ) that will initiate and propagate piping to unstoppable failure. Chapter 2 provides the background for why it is essential to have a predictive methodology for internal erosion by discussing aging infrastructure investment challenges, societal tolerable risk, and the USACE risk assessment process. Chapter 3 will discuss the estimation of seepage gradient from the historical standards through the present with the Sellmeijer and Schmertmann processes. Both the Sellmeijer and Schmertmann methodologies attempt to recreate field conditions in the laboratory. Over the past 20, years the equations have evolved in an attempt to improve and calibrate the methodologies. Chapter 4 will demonstrate the use of the methodologies on two existing projects from different geologic regions of the US to predict the critical reservoir pool level, based on the critical gradient ( $i_{cr}$ ), for piping initiation and progression. Of the two projects, one is located in the Central States and the other is located in the North East. The value for  $i_{cr}$  that is calculated will be used to determine the critical pool levels on the two water impoundment structures (a.k.a. the dams). Comparing the critical pool level to the pool level of record storm events will enable the experts performing the risk assessments to calculate the probability of infrastructure integrity and make informed management decisions. The thesis will conclude with a discussion on the results and suggestions for future considerations in chapter 5.

A lot has been written on the subject of seepage and piping and the methodologies used to predict the behavior of internal erosion. This thesis will provide a concluding look at the behavior and the predictive methodologies in Chapter 5 by comparing and contrasting the two methodologies based on two case studies of existing dam safety projects, and make recommendations on the appropriate conditions of when to use which methodology.

## 1.1 Statistics on US Dam Failure Modes

The Association of State Dam Safety Officials has been compiling statistics on dam failures for the last 40 years. Figure 1.1 illustrates that the seepage and piping failure mode is the second leading cause of dam failures in the United States. This is a serious issue for dam safety engineers who understand the mechanics of piping, but do not fully understand the internal dynamic behavior and the time lag between critical high water events and actual dam failure. The consequences of dam failure can be catastrophe so improving predictive methods for risk analysis continues to be a national priority and the motivation behind this thesis.

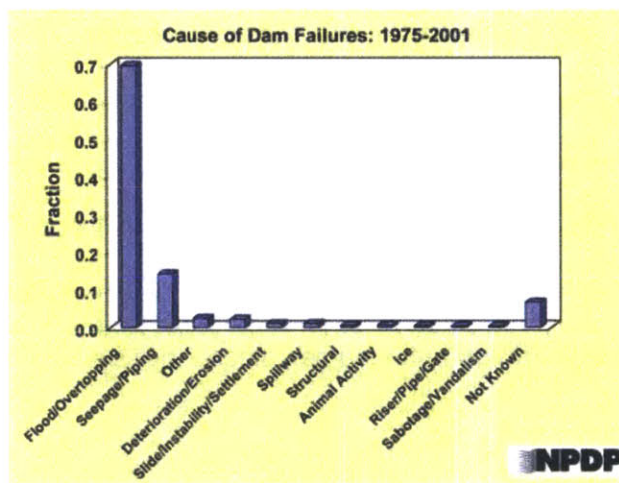


Figure 1.1 National Performance of Dams  
Adapted by: Association of State Dam Safety Officials

## 1.2 Seepage and Piping

Seepage is the movement of groundwater through the porous medium (soil) in response to water pressure measured as hydraulic gradient. The hydraulic gradient ( $i$ ), which can be expressed as  $(\Delta h/L)$  or  $(H/L)$ , is described as the incremental difference of head pressure ( $\Delta h$ ) over a unit of distance ( $L$ ) is expressed in equation 1 (Cherry and Freeze).

$$i = H/L \quad (1)$$

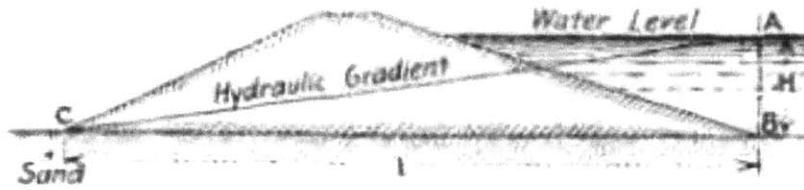


Figure 1.2 Sketch of Hydraulic Gradient and Potential Pipe Path  
From: Bligh, 1910

Figure 1.2 , excerpted from the 1910 Engineering News article written by Bligh, is a visual explanation of the hydraulic gradient for a water impoundment structure. The average head (H) is the difference in water level of the reservoir with reference to the tailwater level (i.e. the difference of elevation at point A and point B). The specific hydraulic head ( $\Delta h$ ) at any point along the potential pipe path is the difference of the water level of the reservoir and the observed water level in a piezometer at a specific point along the pipe path (i.e. along the pipe line between point B and point C). The length (L) a drop of water would have to travel under the structure from the upstream level of the reservoir to the downstream level of the tailwater. L was characterized as the length of “enforced percolation” by Bligh and later the “line of creep” by Lane.

Ground water flows through the soil and is confined within the pore spaces of the soil. The pore water pressure exerted on the individual soil grains by the water flowing through the pore spaces is the seepage force (Watson and Burnett, 1993). Seepage results in the preferential flowpaths from continuous displacement of individual grains of soil by seepage forces, resulting in internal erosion. Figure 1.3 is an illustration of water flow through a dam foundation (i.e. porous medium) and an overview of observations of the onset of seepage and piping at the full scale IJkdijk test at Delft laboratory (Van Beek et al., 2011).

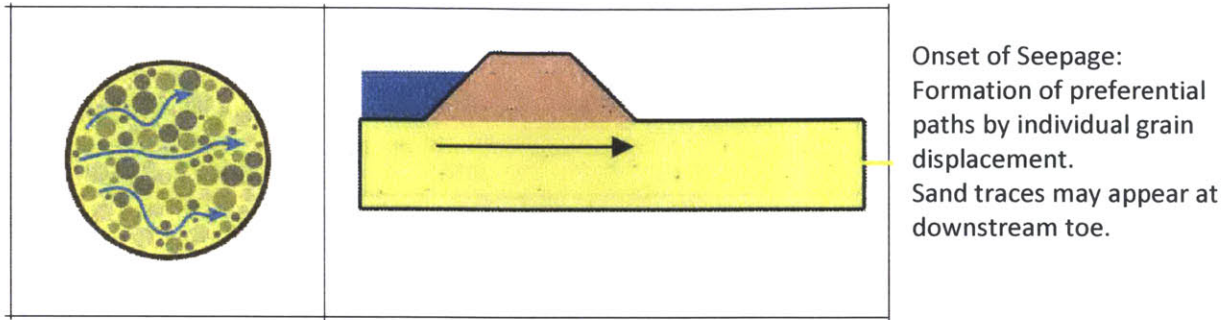


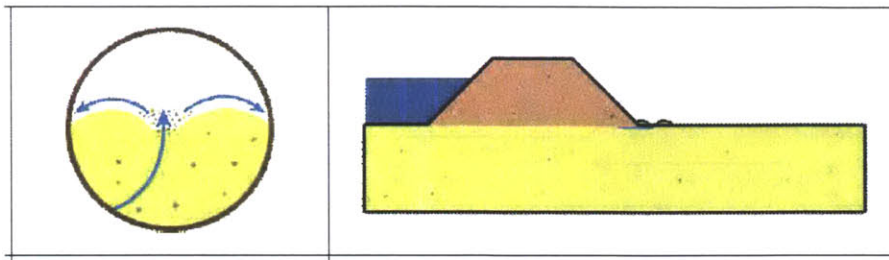
Figure 1.3 Illustration of the Onset of Seepage  
 From: Van Beek et al., 2011

The term piping refers to the development of “pipes” or channels in the soil structure from high seepage forces (Sellmeijer 1988). Piping is a function of velocity induced seepage forces, and velocity can be defined from Darcy’s law with ( $Q$ ) representing seepage flow, ( $v$ ) representing seepage velocity, and ( $K$ ) is permeability of the soil, ( $A$ ) is the cross sectional area of flow, and ( $\Delta h/L$ ) is the hydraulic gradient. Darcy’s law is expressed in equation 2.

$$Q = KA(\Delta h/L) \quad (2)$$

$$v = K(\Delta h/L) \quad (2a)$$

Pipes form when the material is capable of holding and sustaining a roof in order to create a cross sectional area for water to flow. A pipe will progress to the head water of the reservoir and form a larger channel when the critical gradient is reached. The channel may lead to excessive internal erosion and probable failure of the structure. Figure 1.4 is an overview of observations of the onset of piping at the full scale IJkdijk test at Delft laboratory (Van Beek et al., 2011).



Onset of Piping:  
 Sand transporting sand boils  
 form at downstream toe.  
 Piping will continue  
 upstream with a backward  
 progression to create a  
 channel.

Figure 1.4 Illustration of the Onset of Piping  
 From: Van Beek et al., 2011

Dams are usually built in river valleys on alluvial soils with a foundation that extends to some depth ( $D$ ), water is impounded behind the dam, imposing a large differential head (hydraulic gradient) on the foundation soils. A hydraulic gradient is usually present at dams by the nature of difference of water level behind and in front of the dam; therefore, the dam will likely seep (Watson and Burnett, 1993). Engineers can easily calculate the seepage rate ( $Q$ ) using Darcy's law (equation 2) and flownets.

Flow nets are a simplistic two dimensional model based on Darcy's law and are graphical solution of the Laplace equation (Watson and Burnett, 1993). By following accepted rules of steady state flows and the known head conditions, an engineer can anticipate seepage flow and predict seepage pressure. The smallest squares on a flow net are located at points where the flow is concentrated and pressure is high. A flownet is a tool available to the geotechnical engineer to visualize flow, and can be used to predict the behavior of water flow and soil interaction when elevation changes occur in the dam reservoir.

Expected seepage rates are predicted with the use of flownets, or commercial software for more complex flow analysis. Excessive seepage can be observed in the field by the presence of murky water or a "boiling" of sand or fine soil from underground. When boils appear it is an indication that a pipe may be forming inside the structure, and the dam may have a more serious issue under the slope surface that should be investigated and addressed. Sand boils



occur when the seepage pressure becomes greater than the effective weight of the soil this is known as a quick condition (Watson and Burnett, 1993). When quick conditions occur soil particles are floated and the seepage velocities may move the material. The seepage velocities can get so large that they sustain the pipe formation in the soil structure creating a route for water, and subsequent erosion, to flow from the exit point backward in the upstream (upgradient) direction. A localized water pressure decrease in the dam is caused by the pipe growing backward to the reservoir. This behavior was modeled in the Van Beek et al. 2011 study of the influence of relative density on the small scale experiments and shown in Figure 1.5. The lower phreatic line illustrates the reduction in water pressure.

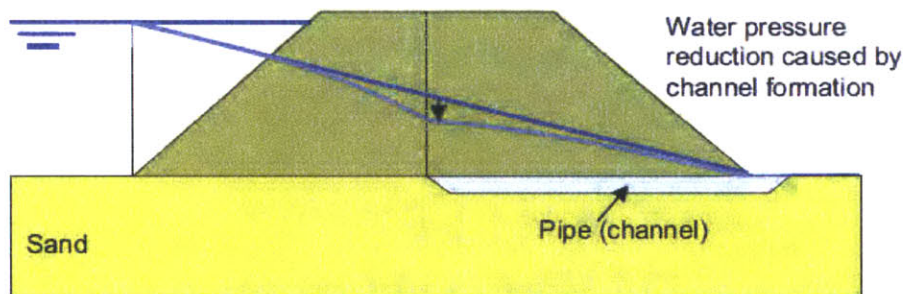


Figure 1.5 Illustration of the Behavior of a Pipe Channel Progression in a Model Simulation  
From: Van Beek et al., 2011

The integrity of a dam is vulnerable when successive sand boils appear indicating that piping initiated and is possibly progressing. The backward progression of the pipe is what is meant by the term piping and it is this critical behavior that jeopardizes the dam. Piping occurs under the surface where one cannot see it happening; this is the reason that the piping mechanism is not perfectly understood by the engineering community and why it is called internal erosion. By the time the signs of internal erosion are evident, it is often too late to intervene. The only way to stop the backward progression of the pipe channel is to lower the gradient by controlling the head differential,  $\Delta h$ , either lowering the reservoir pool or raising the tailwater elevation. Both these remedies are difficult to do during a flood emergency.

Engineers typically focus on the hydraulic gradient in order to reduce seepage velocities when designing remedial measures to mitigate piping issues since this parameter can be more easily engineered than permeability (i.e. the other variable in Darcy's law, equation 2a). Engineers can manipulate the dam geometry, with the knowledge of the soil characteristics, altering the differential head ( $\Delta h$ ) to reduce risk and decrease the vulnerability of the dam. Having a good prediction of the critical gradient that will progress pipe is essential in order to design an effective risk reduction measure.

## 2.0 Background

Aging civil infrastructure offers problems and opportunities to the managing organization. It is helpful to look at the specific infrastructure challenges of one organization to explain why this thesis is interested in understanding the internal erosion mechanism of seepage and piping. The US Army Corps of Engineers (the Corps) has a portfolio of 694 aging dams nationwide, and must maintain them to a safe level of service within a fiscal environment of declining federal resources.

The Corps recognized that there was an opportunity when faced with the knowledge that over 50% of the federal dam infrastructure was reaching its useful service life. Six years ago the USACE addressed the infrastructure challenge by adapting its business model from a solely standards based approach to a portfolio risk management approach to dam safety. The organization transitioned to a nationwide perspective for implementing infrastructure risk reduction projects ([usace.army.mil](http://usace.army.mil)).

The USACE dam safety program made this paradigm shift in 2007 to an enterprise risk management program (ERM). Enterprise risk management in business includes the methods and processes used by organizations to manage risks and seize opportunities related to the achievement of their objectives. ERM provides a framework for risk management that typically involves identifying particular events or circumstances relevant to the organization's objectives (risks and opportunities), assessing them in terms of probability and magnitude of impact, determining a response strategy, and monitoring progress (Wikipedia). The ERM methods and processes will be discussed throughout Chapter 2, including Section 2.3, portfolio risk management: responding to risk within resourcing controls; Section 2.4, Failure mode, effects, and criticality analysis: providing a distinct process for recording the risk assessments results

from the PFMA process; Section 2.4.1, event tree analysis: identifying and quantifying risk; and Section 2.5, Tolerable risk: defining tolerable risk guidelines.

## **2.1 Enterprise Risk Management**

Risk management is a familiar concept when talking about the insurance and financial sectors in the private industry of the US economy. Enterprise risk management (ERM) is a systematic management approach toward risk with a definable framework that focuses management strategies on viewing risk holistically. Implementing ERM is considered a best management practice when managing risk across portfolios. These same strategies and frameworks used in the private industry are applicable to public infrastructure portfolio management. The British, through the National Forum for Risk Management in the Public Sector (Alarm), have provided a good example of successfully implementing risk management processes in public infrastructure. The implementation of ERM processes improved strategic decision making by linking strategic planning with a capital improvement plan at the various governmental levels (i.e. national down to local levels) (AIRMIC, Alarm, IRM: 2010).

There are many opinions regarding what risk management involves, how it should be implemented and what it can achieve. The International Organization for Standardization (ISO) standard 31000 was published in 2009 in response to the need for consistency in defining and implementing enterprise risk management (AIRMIC, Alarm, IRM: 2010). The introduction of the ISO standard has made it a best management practice in organizations across all industries to develop an Enterprise Risk Management (ERM) system. The basic components of enterprise risk management start with a risk aware corporate culture with a defined risk architecture and strategy (AIRMIC, Alarm, IRM: 2010).

The Army Corps has adopted the term portfolio risk management to define the enterprise risk management program that was established six years ago. Figure 2.1 illustrates the generic enterprise risk management process as described in ISO31000. It is a best management practice to develop a risk management process that includes continual feedback loops for adaptation and change as lessons are learned. This concept is illustrated in Figure 2.1 with arrows coming from each of the steps into and out of the Monitor and Adapt, and Communicate and Consult process boxes. The center flowchart is a clear expression of an organization’s risk management principles.



Figure 2.1 Generic Enterprise Risk Management Process  
 After: AIRMIC, Alarm, IRM: 2010

**2.2 Infrastructure Investment Challenges**

The budget for federal spending on civil infrastructure has declined in the last few years. Making do with less is now a part of the federal culture. The complexity of civil infrastructure problems is not limited to funding challenges. Societal behavior is also a challenge. There has

been an increase in development downstream of dams that has dramatically increased the consequences and therefore the risk of dam failure. Tolerable risks will be discussed in section 2.5, but it bears mentioning here that risk reduction measures should be commensurate with tolerable risk guidelines and not all risk require structural solutions. Non-structural solutions such as early warning systems and creating and enforcing zoning regulations within the inundation area of a dam could decrease risk. Figure 2.2 is an F-N cartoon developed by the Army Corps to describe the risk effects in the floodplain after implementing an interim risk reduction measure on a levee system project (USACE 2011). This figure is also applicable for demonstrating the effects of implementing a risk reduction measure on a dam safety project.

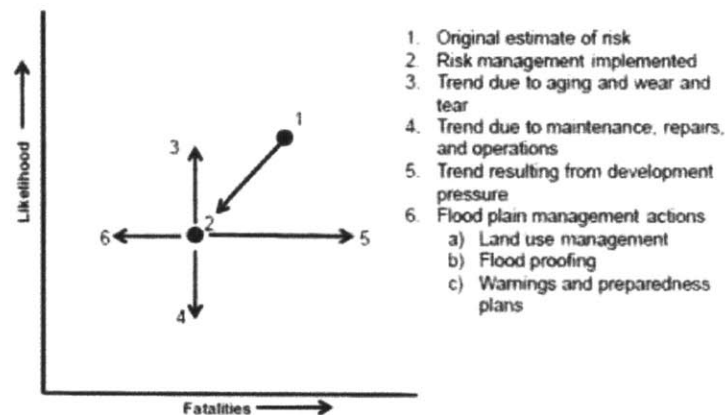


Figure 2.2 Risk Effects in a Floodplain  
From: USACE 2011

Portfolio risk management is the USACE approach to meet the infrastructure challenge. Comparing all projects at a national level, prioritizing projects with a relative ranking, and preparing capital improvement plans based on the relative ranking allows the Agency to invest wisely in the aging infrastructure and to make the largest impact on reducing risk with the limited resources.

## **2.3 Portfolio Risk Management**

Portfolio risk management starts with an inventory and screening level risk assessment of the portfolio to highlight where the projects with the highest risk factors are located. The portfolio projects are ranked relative to one another through a risk informed process of prioritization, and a capital improvement plan was developed. It is very important to get the best prediction of what is influencing the specific project risk during the failure mode, effects, and criticality analysis process, which is described in Section 2.4, so that projects are placed in the appropriate relative rank; this will ensure that the resources are focused on the highest risk projects in a prioritized manner in order to optimize the use of funding.

## **2.4 Tolerable Risk**

The objective of portfolio risk management is to prioritize infrastructure investment in the highest risk projects and to then lower project risk to tolerable levels by meeting project specific “as-low-as-reasonably-practicable” (ALARP) criteria using risk informed decisions (USACE 2011). The concept behind the use of ALARP considerations is that risks lower than the tolerable risk limit are tolerable only if further risk reduction is impracticable or if the cost is grossly disproportional to the risk reduction. ALARP only has a meaning in evaluating risk reduction measures: it cannot be applied to an existing risk without considering the options to reduce that risk (USACE 2011). Figure 2.3 has been excerpted from the USACE 2011 paper entitled *Levee Safety and Tolerable Risk - Implications for Shared Risk, Responsibility, and Accountability* to illustrate how the tolerable risk lines may affect decisions on implementing risk reduction measures. Tolerable risk lines are one piece of the information used by decision makers when relatively ranking projects within the Portfolio and when determining the risk reduction measure to implement for a high risk project. The tolerable risk lines in Figure 2.3 are a helpful illustration for the discussion of the residual remaining risk when evaluating alternative risk reduction measures. Additionally,

portfolio projects that plot above the tolerable risk lines are justified for taking remedial action should funding be available, and portfolio projects that plot below the tolerable risk lines have a diminishing justification for action as the plotted position is located farther down and to the left from the line.

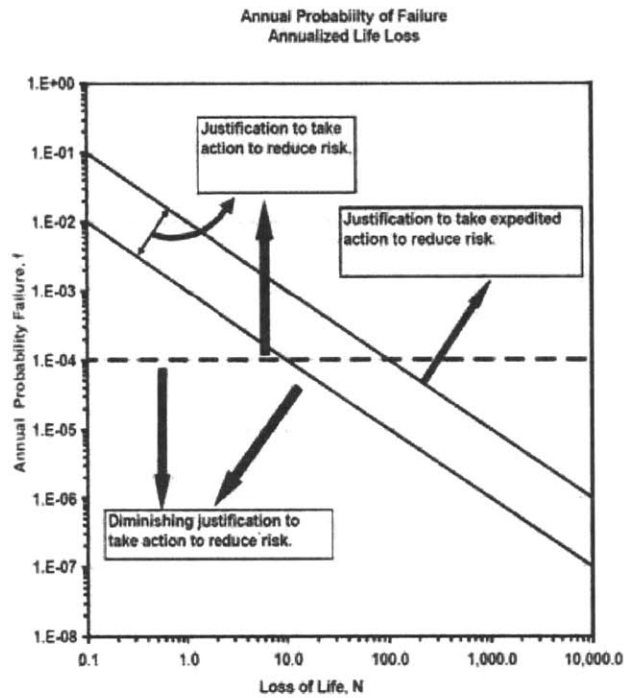


Figure 2.3 USACE Tolerable Risk Guideline  
From: USACE 2011

Should the reader want further explanation of the individual and societal tolerable risks, then he/she is directed to the *U.K. Health and Safety Executive. Reducing Risk, Protecting People, HSE's Decision Making Process*, and the *USACE Dam Safety Policies and Procedures tolerable risk guidelines*, both of which have fully developed the topic of tolerable risk.

Figure 2.4 is a sample set of 25 projects plotted on an F-N chart. The plotted position of each project is based on the probability of project failure (F) vs. the consequences to life if the project



should fail (N). Figure 2.4 was developed for demonstration purposes only. The F-N chart has two diagonal lines that represent individual incremental life safety risk (lower line) and societal incremental life safety risk (upper line).

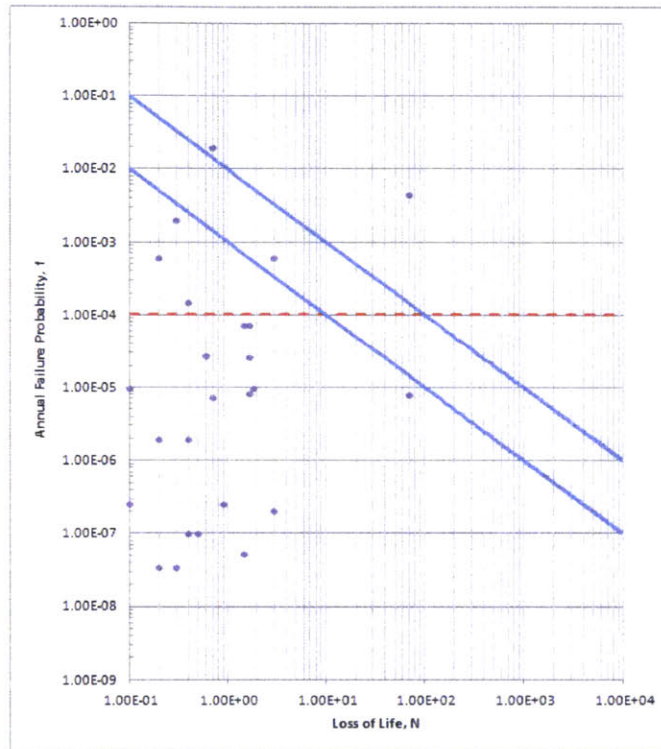


Figure 2.4 Relative Plotting Position of 25 Sample Projects

The project probability of failure is determined through a failure mode, effects, and criticality analysis (FMECA). The FMECA is a qualitative and quantitative assessment of the project and rationale for project placement on the F-N chart.

## 2.5 Failure Mode, Effects, and Criticality Analysis

Failure mode, effects, and criticality analysis (FMECA) was originally developed in the 1950s for the national aeronautics and space administration (NASA) to improve and verify the reliability of space program hardware (Army Technical Manual TM 5-698-4). Failure mode analysis, as

originally conceived by NASA, is used “to evaluate and document the potential impact of each functional or hardware failure on mission success, personnel and system safety, maintainability and system performance. Each potential failure is ranked by the severity of its effect so that corrective actions may be taken to eliminate or control design risk. High risk items are those items whose failure would jeopardize the mission or endanger personnel” (Army Technical Manual TM 5-698-4). The FMECA will: highlight single point failures requiring corrective action, provide a foundation for qualitative reliability, provide estimates of system critical failure rates; provide a quantitative ranking of system and/or subsystem failure modes relative to mission importance (Army Technical Manual TM 5-698-4).

The USACE dam safety program has adopted the FMECA concept, calling it a potential failure mode analysis (PFMA). During the PFMA dam engineers and risk subject matter experts meet at a summit location, once per project, to analyze potential failure modes and predict the probability of occurrence of each failure mode for the specific dam project. The individual probability of failure for each potential failure mode is evaluated using an event tree analysis method, which will be discussed in section 2.4.1. The probability of each potential failure mode is plotted against the consequence of that particular failure mode in an F-N chart (Figure 2.5).

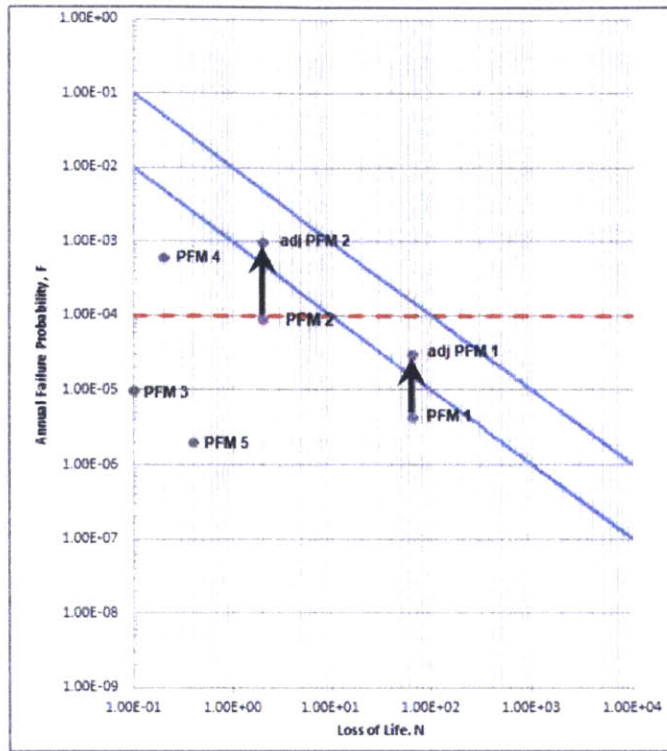


Figure 2.5 Effect of Adjusting the Probabilities of Potential Failure Modes

The F-N graph in Figure 2.5 depicts the plotted position of 5 sample potential failure modes for one project. This schematic graph illustrates the role uncertainty can have when estimating probabilities during the event tree analysis. By adjusting the probability of the potential failure mode 1 (PFM1) higher to the “adj PFM 1” position to reflect greater uncertainty, adj PFM1 crosses over the tolerable risk line (i.e. discussed in Section 2.5). This example is meant to demonstrate the effect that uncertainty can have in estimating the range of probabilities for a failure mode (i.e. the effect of an increase in probability can further translate into an organizational need to consider implementing urgent interim risk reduction measures).

There is a large range of uncertainty in the internal erosion failure mode estimation, and the team of subject matter experts requires a high level of knowledge of the interaction of pore water pressure and soil mechanics to estimate a limited range of probability during the event

tree analysis. The team evaluating each node of the PFM applies significant professional judgment. The effect of uncertainty in the probability assignment during the PFMA is depicted in Figure 2.6.

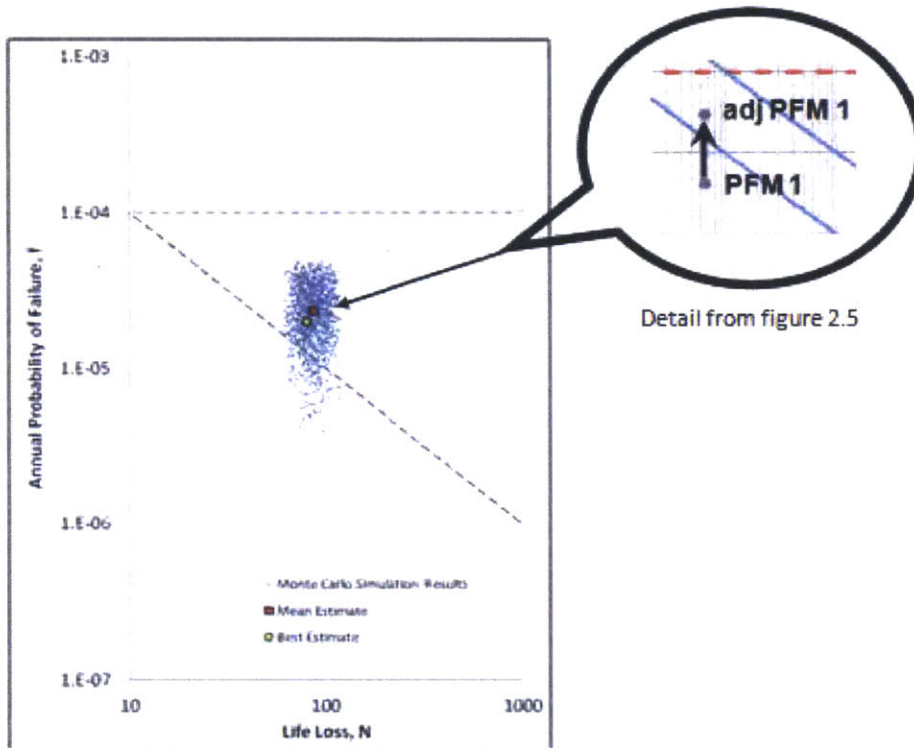


Figure 2.6 Monte Carlo Simulation Determining the Probability of a Potential Failure Mode  
From: USACE 2012

Figure 2.6 was generated with a Monte Carlo simulation and represents the uncertainty, which is shown as scatter, of the estimated probability of one potential failure mode by expert elicitation during the event tree analysis (USACE 2012). The detail of Figures 2.5 and 2.6 illustrate the effect that plotted position. Figures 2.5 and 2.6 demonstrate the importance of uncertainty in estimating probabilities that the management team has to consider when making decisions based on the F-N chart.

The resultant document of the PFMA captures the probability evaluation of each potential failure mode factor that influences the failure behavior in an event tree format. The PFMA includes a quantitative and qualitative narrative of the factors that are represented as individual nodes of the event tree, which is discussed in section 2.4.1.

### **2.4.1 Event Tree Analysis**

The event tree is a tool used by the team of subject matter experts during the PFMA to identify the full sequence of steps required to reach project failure and determine the probabilities of the probable failure modes. The sequence of steps is the failure mode devolved into component events or conditions necessary to propagate failure; in the event tree these events and conditions are called “nodes”. Each node defines one variable that represents an uncertain event (e.g. a boil appears at the toe of the embankment) (USACE 2012).

The team of experts discusses each node describing what specific site conditions would influence behavior and estimate a probability to represent the probability of occurrence of each event or condition. These probabilities are conditional on the occurrence of the preceding events in the tree. The conditional structure of the event tree allows one to compute the probability for any sequence of events by multiplying the probabilities for each branch along a pathway. The branching structure of the event tree originates from a node and is mutually exclusive and collectively exhaustive. The probability for any combination of events (i.e. total failure probability for a potential failure mode) is then computed by summing each branch probabilities across multiple pathways (USACE 2012).

Figure 2.7 is an example of a sub event tree for evaluating the internal erosion failure mode (USACE Dam and Levee Safety Best Practices Manual 2012). A challenge of estimating

probabilities for detailed event trees is remembering that each branch is conditional on predecessor branches. For the typical internal erosion event tree, this means that the probability estimate for the continuation branch should be based on an assumption that the flaw already exists and initiation has already occurred even if the probabilities for a flaw and initiation are very small.

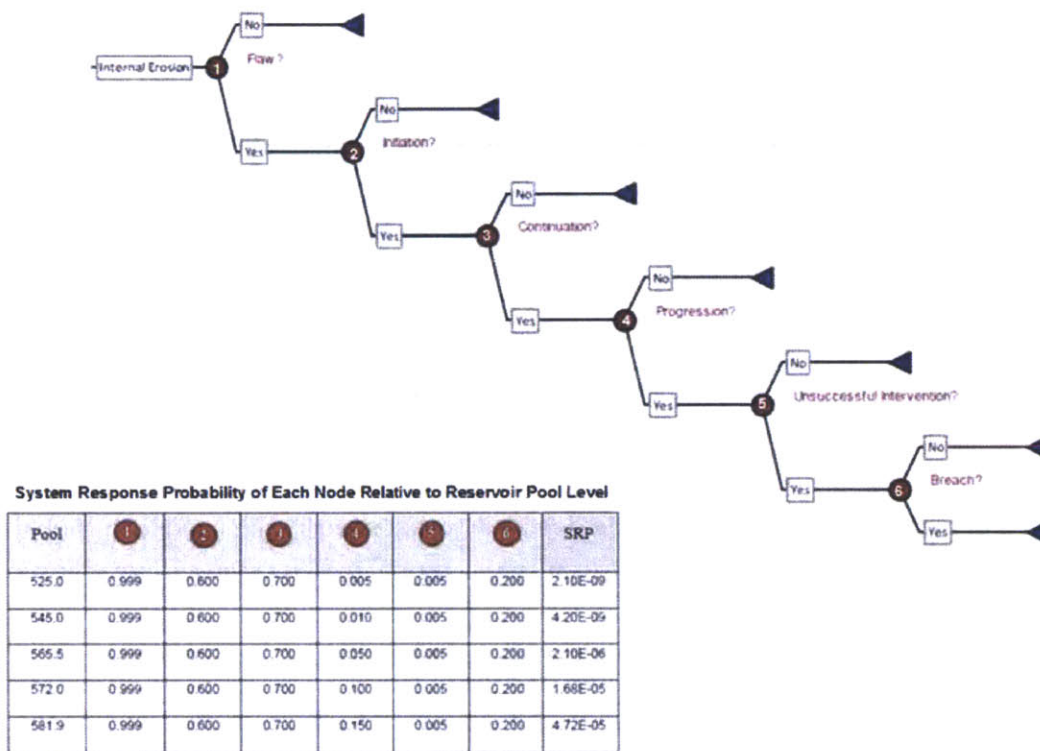


Figure 2.7 Internal Erosion Potential Failure Mode Sub-event Tree  
From: USACE Dam and Levee Safety Best Practices Manual 2012

Overtopping, internal erosion, spillway, slope instability/settlement, and deterioration/erosion of the dam are a few of the potential failure modes that need to be considered in every dam safety PFMA, through event tree analysis. Event sub trees are developed for each of these potential failure modes (PFM) to fully describe the logical progression of events leading to project failure

beginning with the initiating event and continuing through to a set of other events (USACE 2012).

The system response probability (SRP) is dependent on the reservoir pool level as shown in Figure 2.7. The SRP of each potential failure mode (PFM) is estimated and plotted relative to the consequences of failure on an F-N chart when applied to the internal erosion potential failure branch. It is tempting to conservatively estimate probability of failure to over compensate for uncertainty. Doing so can bias the results of the event tree analysis. Understanding the methodology for predicting internal erosion risk is essential to reduce uncertainty in the probability estimate. The more accurate the methodology the better prediction of risk compared to the other better known potential failure modes.





### **3.0 Methods for Determining the Critical Gradient of a Dam**

The serious consequences of sudden dam failure have continually worried engineers and have provided the motivation for understanding the mechanisms of failure. One of the most serious and most difficult mechanisms of failure to conceptualize is internal erosion through piping. Engineers have been offering opinions on predicting critical gradients to develop a factor of safety against a piping failure for the last 100 years using empirical data and laboratory experiments to study the mechanisms of piping. A common theme in the refinement of determining the factor of safety against piping is to develop a reasonable predictive methodology for determining the potential critical gradient that initiates and propagates piping. A secondary goal is to limit conservatism in the critical gradient calculation in order to build economical structures. The term “methodology” is used to represent the different authors’ processes for determining the critical gradient of a water impoundment structure (i.e. dam). The methodologies are informed through the use of a single or multiple equations.

Over time researchers have attempted to improve the predictive methodologies by empirical and experimental means. Researchers have built models and flume tests to reconstruct scaled visualizations, in an effort to examine physical properties of the piping mechanism. The first design rule for determining a factor of safety for the design of safe dams was presented by Bligh (1910). Many engineers have studied the piping phenomena in dams and offered methodologies for predicting internal erosion triggers; however, this thesis will only discuss a few methodologies.

### 3.1 Bligh

W.G. Bligh presented a paper *Dams, Barrages, and Weirs on Porous Foundations* (Bligh, 1910) to explain the principles underlying safe design practices for hydraulic impoundment structures (i.e. dams and weirs) founded on porous materials. The paper was the first design rule for dam safety engineering practice. Bligh formulated the “reliable” design rule by analyzing a number of disastrous dam failures in India. Bligh was the first to write about the equilibrium of forces on the soil by referencing the counterbalance of upward seepage pressure and the hydrostatic forces of the dam structure. He described the micro-interactions of the water and the soil as the velocity of the water moving through a pipe that had formed in the porous foundation, which is directly proportional to the hydrostatic pressure (i.e.  $\Delta h$ ) and inversely proportional to the length of “enforced” percolation that the water travels under the impoundment structure ( $L$ ) (Bligh, 1910). Bligh considers the percolation through the foundation of a dam as enforced by the self-weight and impermeable character of the dam embankment. He further explains that a piping situation in the foundation can be stopped or “neutralized” by the friction encountered by the “slow percolating current” (i.e. low seepage velocities will not form a sustainable pipe).

By analyzing the various dam foundation materials in the Indian case studies Bligh recognized that dams are subject to hydrostatic pressures that vary with respect to soil type. Bligh thought the safety of masonry dams depended on the length of the percolation path through the soil medium, which he defined as the length the water droplet has to travel below the structure (i.e. the length of the enforced percolation  $L$ ), relative to the hydrostatic pressure exerted on the water droplet (i.e. the change in head elevation  $H$  from the reservoir to the tailwater).

Referencing Figure 1.2 Sketch of Hydraulic Gradient and Potential Pipe Path of Section 1.2,  $L$  is the distance from point B to C, and  $H$  is the elevation change from point A to C. Bligh developed the percolation factor ( $c$ ) through empirical analysis based on the characterization of

the foundation soil. Bligh believed an engineer could design a safe dam if he followed the design rule of equation 3.

$$L = c H \quad (3)$$

The two important concepts that Bligh introduced to the practice of dam safety engineering were the systematic response of a dam to a hydraulic gradient and the dependence of that response to the characteristics of the foundation soil. The percolation factors for the various soils as defined by Bligh are listed in table 1 of Section 3.3, and will be discussed further in Section 3.3.

### **3.2 Terzaghi**

In 1928 Terzaghi wrote a paper on *The Effect of Minor Geologic Details on the Safety of Dams* (Terzaghi, 1928, in English). He wrote that the most important danger that threatens dams that are founded on unconsolidated alluvial fills was the existence of piping. Piping as Terzaghi defines it is “water forcing its way from the storage reservoir through the underground towards the tail race”. The 18 years leading up to Terzaghi presenting this paper found the engineering community using the percolation coefficient introduced by Bligh in 1910 to calculate a factor of safety against piping. Terzaghi thought the “percolation coefficient represents a rather crude empirical conception without direct relation to physical standard of units” (Terzaghi; 1928). Terzaghi thought an empirical rule based solely on statistics did not lead to a standard factor of safety calculation. Terzaghi strongly cautioned that practicing engineers should be fully aware of the specific geologic conditions of their sites and consider the minor geologic details along with the grain size of the foundation materials beyond the use an empirical percolation coefficient.

Terzaghi was interested in knowing more on the physical factors that lead to piping, so he constructed flownets and built a model to investigate the piping mechanism in order to test the Bligh assumption that the critical head depends only on grain size (i.e a percolation coefficient related to grain size only). Concentrating on theoretical hydrodynamics, he was interested in the head when the upward pull of flowing water (seepage) exceeded the downward pull of the gravity forces. The test results of the physical model showed that the percolation coefficient is only one of several factors that should be considered when calculating the critical gradient and factor of safety against piping. Terzaghi found the strongest influence on the critical reservoir level was the maximum hydraulic gradient,  $i_{max}$ , at which the water flows out of the ground (i.e. the exit gradient). The  $i_{max}$  can vary widely depending the cross section selected for the foundation (Terzaghi 1928); this concept was incompatible with Bligh's rule. Terzaghi determined that the seepage force ( $p_s$ ) acting at the danger point is equal to the unit weight of water,  $\gamma_w$ , multiplied by  $i_{max}$ , which is expressed in equation 4 .

$$p_s = i_{max} * \gamma_w \quad (4)$$

In 1948 Terzaghi partnered with R. Peck to write the book *Soil Mechanics in Engineering Practice* (Terzaghi and Peck, 1948). Terzaghi and Peck determined that the critical hydraulic gradient occurs when the effective stress becomes equal to zero at any depth in the layer of sand (i.e. the average seepage pressure becomes equal to the submerged weight of the sand). Equation 4 evolved into equation 5 for the critical gradient,  $i_{cr}$  , which is equal to the buoyant unit weight of the soil divided by the unit weight of water.

$$i_{cr} = \gamma_b / \gamma_w \quad (5)$$

Equation 5 has continued to be the essential formula for predicting critical gradient for the last 65+ years.

### 3.3 Lane

In 1934, E. W. Lane (Lane, 1934) concluded a study into the seepage under dams and presented his work to the American Society of Civil Engineers (ASCE). The first of two papers that Lane presented to the ASCE was the *Security from Under-Seepage, Masonry Dams on Earth Foundations*. Lane introduced a new method of dam safety analysis based on his investigation into the conditions of more than two hundred dams in India. Through empirical analysis, he offered a refinement to the length of percolation path as defined by Bligh. Lane suggested that soil is more resistant to seepage in the vertical direction than the horizontal. Lane introduced the important concept of the systematic response of dam foundation seepage to anisotropic soil conditions to the practice dam safety engineering. The refinement to the Bligh percolation design rule generally permits the use of smaller percolation distances (i.e. a smaller cross sectional area of the dam).

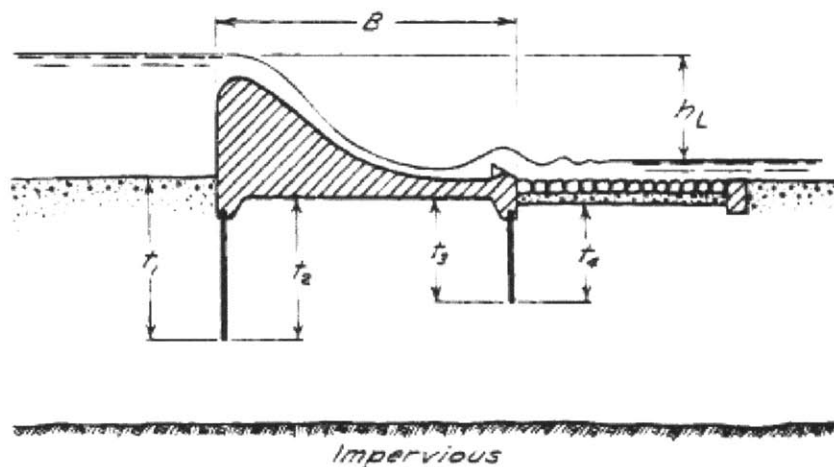


Figure 3.1 Flow Path of an Idealized Water Molecule under the Dam  
From: Terzaghi, et al., 1996

To address anisotropic conditions of the soil, Lane estimated that one could reduce the vertical distance an idealized water particle travels by 1/3 compared to the horizontal distance that the same water drop travels to the exit point. Lane recognized that the 1/3 ratio developed through

the empirical analysis may not be the best possible ratio for all situations, and suggested further study to develop a reliable ratio. Figure 3.1 is an illustration of a foundation cross section (with sheet pile cutoffs) to aid in visualizing a path that an idealized drop of water would flow through the foundation when propelled by a hydraulic gradient, as envisioned by Lane and presented by Terzaghi, et al. (Terzaghi, et al., 1948, 1996). The vertical distance an idealized drop of water would travel is symbolized by  $t$  and the horizontal distance that same drop of water would travel is symbolized by  $B$ .

$$C_w = \frac{\frac{1}{3}B + \sum t_i}{h_{cr}} \quad (6)$$

Through empirical methods, Lane specified the weighted creep ratio for each soil category, which are listed and compared to the original percolation factor defined by Bligh in Table 1.

Table 1 Comparison of Weighted Creep Ratios

Soil type	Lane $C_w$	Bligh $c$
Very fine sand or silt	8.5	18
Fine sand	7.0	15
Medium sand	6.0	
Coarse sand	5.0	12
Fine gravel	4.0	
Medium gravel	3.5	
Gravel and sand		9
Coarse gravel, including cobbles	3.0	
Boulders with some cobbles and gravel	2.5	
Boulders, gravel, and sand		4 to 6
Soft clay	3.0	
Medium clay	2.0	
Hard clay	1.8	
Very hard clay, or hardpan	1.6	

To determine the vertical factor of 1/3, Lane analyzed data from the Indian dams. Specifically, Lane characterized the dams by soil type and separated the dams that failed from the dams that did not fail in each soil category. Figure 3.2 displays a subset of the Indian case studies used in

Lane's analysis (i.e. the sand, fine sand, and silt category). The  $H \approx 3V$  trend line in the sand data is aligned along the six dam failures in this category. There are a few dams that did not fail below this "unsafe" line so it is unclear how he analyzed the trends of failure and the commonality among the dams that failed and those that did not fail. However, the deduction that the horizontal creep distance is not as effective in resisting piping as the vertical creep distance intuitively makes sense, and the trend line in Figure 3.2 possibly provides a rationale for the factor of 1/3. This fraction roughly corresponds to a  $k_h$  to  $k_v$  ratio of 3. We know today that sedimentary soils are often less permeable in the vertical direction than the horizontal direction and that dam foundations are often comprised of sedimentary deposits.

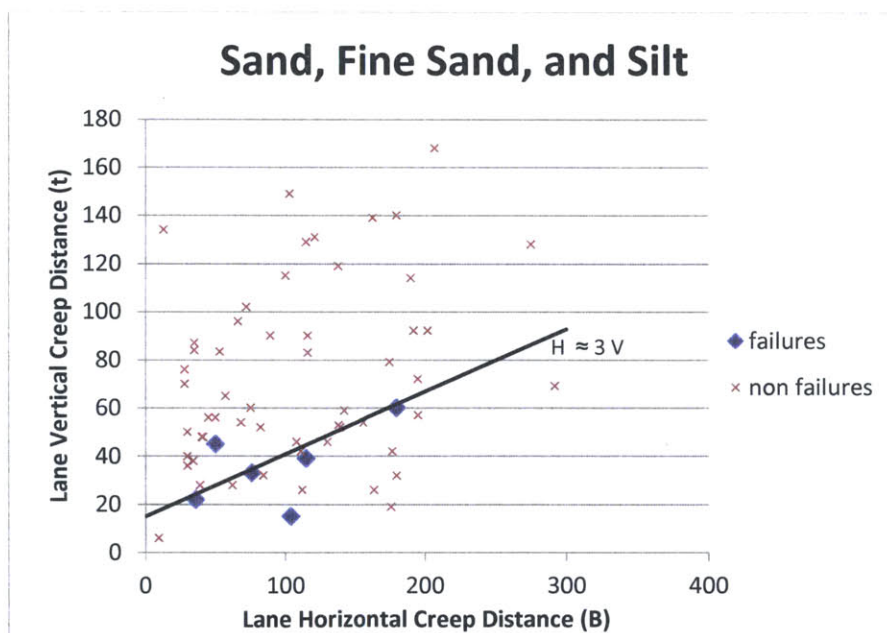


Figure 3.2 Subset of Lane Data for Sand, Fine Sand, and Silt  
After Lane, 1934

### 3.4 Sellmeijer

J. Sellmeijer initially introduced a predictive design rule for the critical gradient of a water impoundment structure in his PhD thesis *On the mechanism of piping under impervious*

*structures* (Sellmeijer, 1988). Like Terzaghi before him, Sellmeijer considered all aspects of piping. In his 1988 PhD thesis, Sellmeijer fully considered the soil mechanics of piping and analyzed the equilibrium of forces on the individual sand particle to predict the critical gradient of a structure, based on its geology and geometry, beyond which a pipe would propagate through the foundation from the tailwater to the headwater of the reservoir (Sellmeijer, 1988). In 1993, Sellmeijer and J. Weijers (Sellmeijer and Weijers, 1993) presented a paper *A new model to deal with the piping mechanism* describing the laboratory experiments that were conducted in Delft, Netherlands, on the piping mechanisms of embankments to test the predictive rule presented in the PhD thesis. Together with Weijers, Sellmeijer built a flume of specific dimensions (0.5 x 0.3 x 0.1m) and tested various scenarios to determine if an obvious rule could be formulated to predict the critical gradient that initiates and subsequently progresses a piping failure.

Equation 7 was presented in the 1993 Sellmeijer and J. Weijers paper (Sellmeijer and Weijers, 1993). The input parameters for equation 7 are further refinements on the basic inputs defined by Bligh (Bligh, 1910).  $H_{crit}$  is the critical head above which the internal erosion of a dam becomes progressive in a dam. Equation 7b is Sellmeijer's interpretation of the percolation factor  $c$ , which includes the soil characteristics  $d_{70}$ , a representative soil size,  $L$ , the length of enforced percolation, and  $\kappa$ , the intrinsic permeability of the soil.  $D$  is the depth of the foundation soil that is susceptible to piping, and  $\Theta$  is the bedding angle of the soil that is also known as the angle of internal friction of the soil particles, and the densities of the test soil and of water are designated by  $\rho_p$  and  $\rho_w$  respectively. Equation 7a is the depth to length ratio with scaling factors to correlate flume geometry to real project conditions.

$$H_{crit} = \alpha c \frac{\rho_p}{\rho_w} \tan \theta (0.68 - 0.10 \ln c) L \quad (7)$$



$$\alpha = \left(\frac{D}{L}\right) \left(\frac{0.28}{\left(\frac{D}{L}\right)^{2.8} - 1}\right) \quad (7a)$$

$$c = \eta \left[ \frac{d_{70}^2}{\kappa} * \left(\frac{d_{70}}{L}\right) \right]^{1/3} \quad (7b)$$

Figure 3.3 is an illustration of the geology input parameters for equations 7 through 7b.

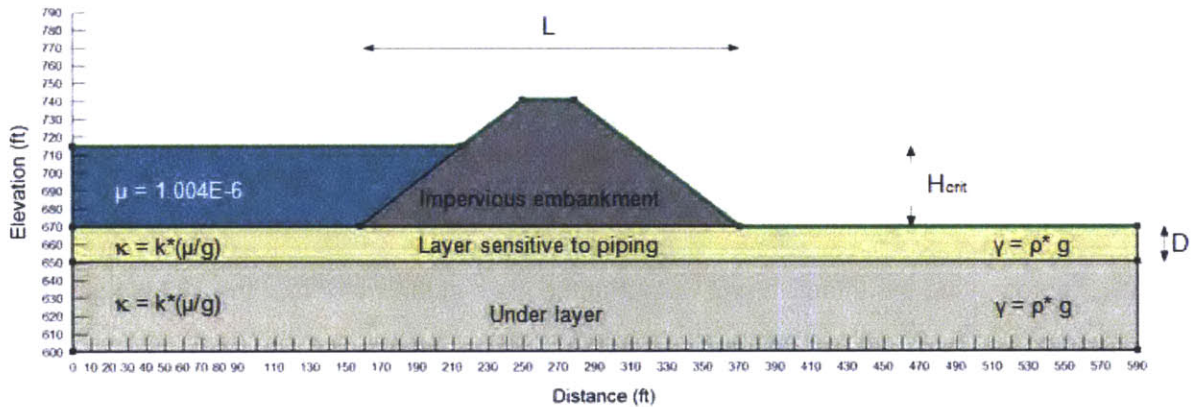


Figure 3.3 Visual Representation of the Parameters Used in Sellmeijer Methodology

A description of the parameters used in the Sellmeijer Methodology that are expressed in equations 7 – 7b is provided in Table 2 .

Table 2 Sellmeijer Methodology Input Parameters

Input Parameter	Description of Parameters
L	length of enforced percolation under the dam.
D	depth of the soil layer sensitive to piping.
$\rho$	density of the soil layer.
$\rho_w$	density of water.
$\theta =$	angle of repose (i.e. bedding angle) is often considered equal to the angle of internal friction of the soil particles for loose material.
$\kappa$	intrinsic permeability is the permeability that is associated with Darcy's law. It is a function of the soil unit weight ( $\gamma_p$ ), permeability (k), and $\mu$ , the constant that represents the viscosity of fluid dependent on the ambient temperature of the case being analyzed.
$d_{70}$	representative grain size is a soil property that represents 70% of the

	grain size distribution of the soil passing through a sieve in a sieve analysis.
$\eta$	White's constant was deduced by C. White 1940 based on his analysis of the equilibrium of grains on the bed of a stream (White, 1940).

Equation 7 was developed as a predictive rule and is based on the equilibrium forces on a sand particle. Sellmeijer used White's constant,  $\eta$ , in equation 7 to account for the substantial open space between the top grains (Sellmeijer, 2006). C. White originally defined  $\eta$  (White, 1940) as the packing coefficient to describe the closeness of the grains while he was examining the equilibrium of the individual sand grains with respect to tangential stresses. Figure 3.4 (Sellmeijer, 2006) illustrates the balance between the force along the sloping channel and the vertical force. It is based on a similar diagram sketched by White, and excerpted from the Sellmeijer, et al. (2006) with  $p$ ,  $a$ , and  $\alpha$  representing the erosion channel (i.e. the pipe) gradient, height, and angle;  $d$  representing the particle diameter;  $\alpha$  representing the bedding angle; and  $\gamma_p'$  and  $\gamma_w$  representing the effective unit weight of the grain in the water and the unit weight of water respectively.

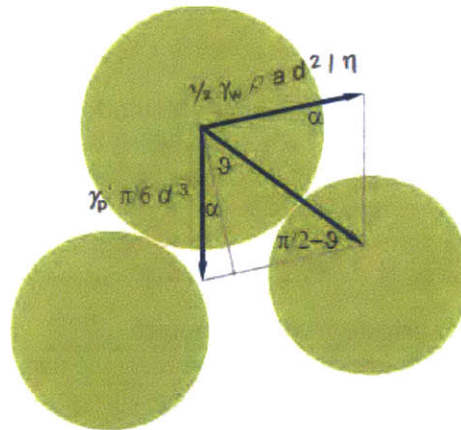


Figure 3.4 Two Force Balance of a Top Grain  
From: Sellmeijer, 2006

Sellmeijer further refined the prediction rule based on the forces on the sand grains with the additional consideration of the flow in the pipe that forms in the aquifer (Van Beek, 2010). The

Sellmeijer methodology has grown in sophistication over the last 20 years. Multiple flume tests and large scale field tests have been repeated in order to verify and validate assumptions and improve the scale factors to overcome bias introduced by the geometric limitations and confining pressures of the smaller flume test. Van Beek et al. (2010) further used a multivariate analysis to validate and refine the input parameters. The culmination of the refinements to the Sellmeijer's prediction rule developed in 2011 is represented by Equation 8. Sellmeijer adjusted the structure of equation 7, and the input parameters were grouped into three meaningful clusters,  $F_R$ , the resistance factor shown in equation (8a),  $F_S$ , the scale factor shown in equation (8b), and  $F_G$ , the geometrical shape factor shown in equation (8c). Equation 8 introduced three new soil parameters that include KAS, RD, and U and use unit weight ( $\gamma$ ) rather than density ( $\rho$ ) to of soil and water. The three new parameters introduced in the FR term are normalized by the mean value of the calibration experiments, which is designated by a subscript "m" on KAS, RD, and U, thus making the parameters dimensionless in equation 8a.

$$i_{cr} = \frac{H_c}{L} = \frac{1}{c} = F_R F_S F_G \quad (8)$$

$$F_R = \eta \frac{\gamma_p}{\gamma_w} \tan \theta \left( \frac{RD}{RD_m} \right)^{0.35} \left( \frac{U}{U_m} \right)^{0.13} \left( \frac{KAS}{KAS_m} \right)^{-0.02} \quad (8a)$$

$$F_S = \frac{d_{70}}{\sqrt[3]{\kappa L}} \left( \frac{d_{70}}{d_{70,m}} \right)^{0.60} \quad (8b)$$

$$F_G = 0.91 \left( \frac{D}{L} \right) \left( \frac{D}{L} \right)^{\frac{0.28}{2.8} - 1} + 0.04 \quad (8c)$$

A description of the additional parameters used in the Sellmeijer Methodology that are expressed in equations 8 – 8bc is provided in Table 3.

Table 3 Additional Sellmeijer Methodology Input Parameters

Input Parameter	Description of Parameters
$\gamma_p$	unit weight of the soil layer sensitive to piping (i.e. $\gamma_p = \rho_p g$ ). Unit weight, which is a force, is introduced to replace $\rho$ term.
$\gamma_w$	unit weight of water (i.e. $\gamma_w = \rho_w g$ ). Unit weight, which is a force, is introduced to replace $\rho$ term.
RD	relative density is a measurement of how tightly the particles are packed together relative to how tightly the particles could potentially pack together given the soil characteristics. It is an indication of the porosity of the soil (i.e. the amount of interlocking for a given void ratio).
U	Uniformity coefficient is an indication of how well sorted the soil layer is, which effects how the individual soil particles are able to pack together. It is the degree of uniformity in the granular material based on the grain size distribution of a soil sample. The alignment or packing will influence the strength, compressibility, and permeability of the soil.
KAS	angularity (i.e. roundness) of the soil particles. Geometry of the soil particles helps define the ability of the soil to pack together. This parameter is included to account for the effect of frictional resistance on the micro scale of particle interactions. One would expect angular particles to interlock more effectively.

The Sellmeijer corrective factors for resistance ( $F_R$ ), scale ( $F_S$ ) and geometry ( $F_G$ ) are meant to relate the experimental test results to real project conditions. The resistance factor ( $F_R$ ) expresses the equilibrium of forces on the soil particles within the foundation; the parameters are particle roundness, unit weight of the particle compared to the unit weight of water, relative density, uniformity and White's constant, (KAS,  $\gamma$ , RD, U,  $\eta$ ).

The angularity of the soil particles (KAS) is difficult to estimate on existing projects since samples must be visibly inspected to subjectively determine the value of KAS. However, Van Beek et al. (2010) determined through analysis that the KAS parameter has very little influence on equation 8.

The scale factor ( $F_S$ ) relates the grain size to the total dam length (i.e. seepage length) using the grain size, permeability, and creep length parameters ( $d_{70}$ ,  $\kappa$ , and L). The wider the dam

(greater L) the less erosion should occur because the water will encounter more resistance of the soil. The permeability and the grain size both have a strong influence on equation 8. The Sellmeijer methodology does not directly address the possibility of anisotropic foundation conditions; although, a recent study by Van Beek et al. (2012) analyzed the potential influence of the permeability of the layer under the primary piping layer. There is potential for adapting Sellmeijer's equation 8b to account for anisotropic soil conditions by modifying the  $F_s$  scaling factor according to the Van Beek et al (2012) analysis. The Sellmeijer methodology had a large variation (up to 25%) in results when the coarser sand (i.e.  $d_{70} = 200 \mu\text{m}$ ) was tested. For this reason, it is suggested that the equation be used for soil within the calibrated range only, which corresponds to values of  $U < 3$  (Sellmeijer 2011).

The geometry factor ( $F_G$ ) relates the depth to length ratio of the layer sensitive to piping to the groundwater flow. This factor is the most complex, and is what engineers have been struggling to understand since Bligh and Lane first wrote on the subject of seepage and piping under water impoundment structures.

Sellmeijer's early work and equation 7 were limited to relationships of water flow with the media in the flume. The latest equation 8 is an appreciable improvement including some of the minor geology details of real projects, as Terzaghi suggested 85 years ago. The Sellmeijer methodology includes the necessary corrections to relate laboratory tests to real field conditions in three categories (i.e.  $F_R$ ,  $F_S$ ,  $F_G$ ) making it appear to be a simple methodology to follow.

Sellmeijer's equation 8 is the methodology that will be used to compare with the Schmertmann methodology.

### 3.5 Schmertmann

J. Schmertmann (2000) was interested in providing a rational analysis of the piping phenomenon through flume testing and a simplified theoretical underpinning through flownets. In 2000, Schmertmann presented the paper *The No-Filter Factor of Safety Against Piping Through Sands* (Schmertmann, 2000). Familiar with Sellmeijer's work at the Delft Hydraulics Laboratory, Schmertmann designed and supervised a similar series of flume tests at the University of Florida (UF). The UF flume (8' x 1' x 1') was built to different dimensions than the Delft lab flumes. Schmertmann was interested in creating results that were comparable to the Sellmeijer flume results in order to produce a simplified rule to determine a factor of safety in dam design based on the critical gradient. Schmertmann relied on the use of flownets in conjunction with the results of the flume tests at both the University of Florida and the Delft Lab to develop his methodology. Schmertmann based his work on Sellmeijer's original equation 7.

Equation 9 is the Schmertmann Methodology (Schmertmann, 2000) for determining the factor of safety (FS) of dam system response against the initiation of backward erosion of a water impoundment structure (i.e. a dam). The term  $F_{px}$  is the factor of safety calculated at any point along the pipe flow path. The term  $i_{pmt}$  is the key input parameter in equations 9 and 10.  $i_{pmt}$  is the maximum point seepage gradient needed for a complete pipe to form in the UF flume test series. The term  $i_x$  is the seepage gradient at any point  $x$  along the pipe flow path in the field (i.e. the dam). The remainder of the terms are correction factors. Schmertmann deduced correction factors in order to relate the flume test results to the geology and geometry of real project conditions.  $C_D$ , is the correction factor for (D/L),  $C_L$ , is the correction factor for total pipe length  $L$ ,  $C_R$ , is the correction factor for dam axis curvature,  $C_S$ , is the correction factor for grain size,  $C_z$ , is the correction factor for high-permeability under layer,  $C_a$ , is the adjustment for pipe

inclination,  $C_\gamma$ , is the correction factor for density, and  $C_K$ , is the correction factor anisotropy.

The correction factors are applied to  $i_{pmt}$  to determine the Factor of Safety (FS).

$$F_{px} = \frac{(C_D C_L C_S C_K C_Z C_\gamma) i_{pmt} (C_\alpha)}{C_R i_{tx}} \quad (9)$$

The seepage gradient  $i_{tx}$  is  $i_{cr}$  when FS=1; this is the critical condition for the dam. The factor of safety value of 1 is entered into the Schmertmann equation 9 and the equation is rearranged to calculate for the critical gradient,  $i_{cr}$ . Equation 10 is the rearrangement and represents the critical gradient for which the calculated results will be compared in Chapter 4.

$$i_{cr} = [(C_D)(C_L)(C_S)(C_K)(C_Z)(C_\gamma)(C_\alpha) / C_R](i_{pmt}) \quad (10)$$

$$C_D = \frac{\left(\frac{D}{L_f}\right) \left(\frac{\left(\frac{D}{L_f}\right)^{2.0} - 1}{0.20}\right)}{1.4} \quad (10a)$$

$$C_L = (L_t / L_f)^{0.2} \quad (10b)$$

$$C_S = (d_{10f} / 0.20 \text{ mm})^{0.2} \quad (10c)$$

$$C_K = (1.5 / R_{kf})^{0.5} \quad (10d)$$

$$C_Z \text{ determined from chart in Appendix G} \quad (10e)$$

$$C_\gamma = 1 + 0.4(D_{rt} / 100 - 0.6) \quad (10f)$$

$$C_\alpha = i_{p\alpha} / i_{po} \quad (10g)$$

$$C_R = (R_1 + R_0) / R \text{ for a curved dam axis} \quad (10h)$$

A description of the parameters used in the Schmertmann Methodology that are expressed in equations 10 – 10h is provided in Table 2 .

Table 4 Schmertmann Methodology Input Parameters

Input Parameter	Description of Parameters
D	depth of foundation layer sensitive to piping.
$L_f$	direct length (not meandered) of the ends of a possible pipe path measured on a transformed section of a flownet. A transformed flownet is based on the anisotropic soil properties.
$L_t$	length of pipe in the flume test.
$d_{10f}$	representative grain size of the field soil property that represents the equivalent grain size with 10% of the grain size distribution smaller by weight.
$R_{fk}$	representation of anisotropic conditions in the field by relating the horizontal permeability to the vertical permeability of the soil ( $k_h/k_v$ ).
$D_{rf}$	relative density of the field soil is a measurement of how tightly the particles are packed together relative to how tightly the particles could potentially pack together given the soil characteristics. It is an indication of the porosity of the soil.
$i_{po}$	field horizontal gradient obtained by applying all correction factors, except $C_\alpha$ , to $i_{pmt}$ .
$i_\alpha$	field critical gradient as a function of the angle of inclination of the pipe (i.e. if not horizontal) and $i_{po}$ .
R	Radius to a point on the pipe path in a dam with a curved axis, as measured along the centerline of the horizontal curve.
$R_1$	Shortest radius to an end of a completed path, as measured along the inside arc of the horizontal curved boundary of the dam.
$R_0$	Longest radius to the end of a completed path, as measured along the outside arc of the horizontal curved boundary of the dam.

The maximum point gradient needed to complete the pipe,  $i_{pmt}$ , in each of the University of Florida (UF) and the Delft Laboratory flume test experiments is plotted against the  $C_u$  ( $d_{60}/d_{10}$ ) of each test in Figure 3.5 (Schmertmann, 2000). Figure 3.5 presents the combined data set (i.e. Delft tests (71 points) and the University of Florida (37 points)). Schmertmann created the larger data set to provide rigor to his methodology. Unfortunately, Schmertmann did not design the UF flume test to the same dimensions as the Delft flume. To account for the difference in flume geometry, Schmertmann back calculated consistent geometries between the differently scaled test apparatuses in order to produce the more complete data set of figures 3.5 and 3.6. This data was plotted to provide a look-up graph for Equations 9 and 10.



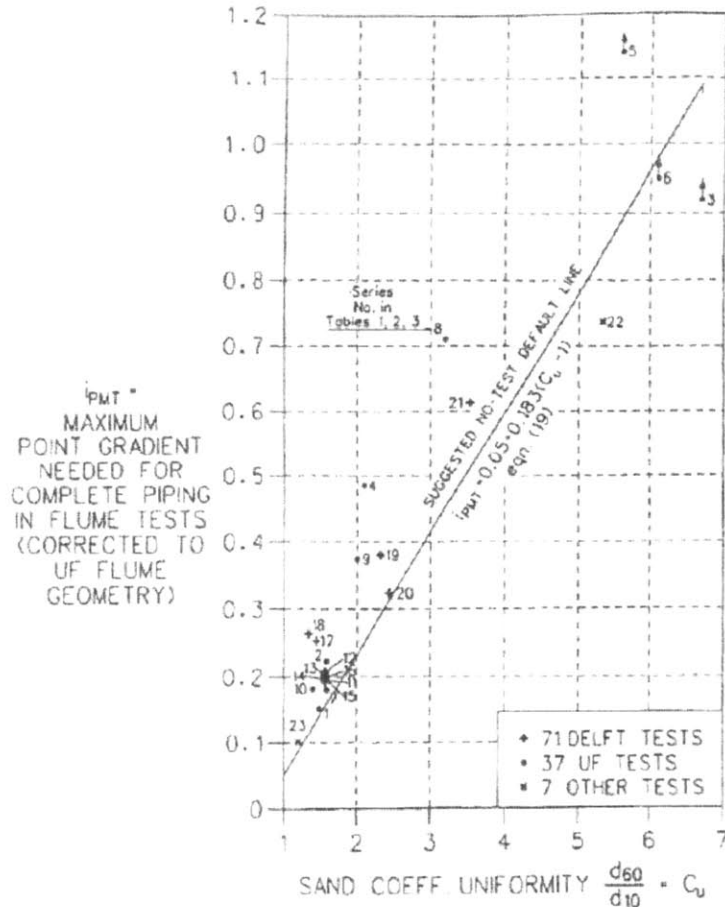


Figure 3.5 Schmertmann Correlation for Determining  $i_{pmt}$   
From Schmertmann, 2000

The linear relationship of Figure 3.5 does not intuitively make sense. It suggests that for high  $C_u$  values the  $i_{pmt}$  will be very large, and the calculated critical gradient,  $i_{cr}$ , will be much larger implying a critical reservoir pool elevation that is much higher than the physical dam. In other words the critical gradient is solely determined by the uniformity coefficient of the soil. The data set of 108 test results (Schmertmann, 2000) were plotted to create Figure 3.6. As illustrated in Figure 3.6 the data more closely relate to the uniformity coefficient ( $C_u$ ) with a polynomial function (with a  $R^2$  value of 0.922) rather than a linear function (with a  $R^2$  value of 0.847). The

polynomial curve fit produces a more logical relation for this limited data set, meaning that at higher  $C_u$  values the  $i_{pmt}$  would eventually reach a max value such as 1.0. A broader range of  $C_u$  tests would provide insight as to what a more appropriate  $(i_{pmt})_{max}$  should be. Experience leads this author to think the behavior of a broader data set would display a logarithmic behavior, but for now the limited  $C_u$  test range, which displays the polynomial behavior of Figure 3.6, is the best information to work with. In an effort to fully evaluate the methodology, the polynomial function shown in Figure 3.6 will be used as the  $i_{pmt}$  relation to determine the  $i_{cr}$  value. To produce results for the comparison between the Schmertmann and Sellmeijer methodologies  $i_{pmt} = 1$  will be used for soils with a  $C_u > 6$  with the caveat that the “fixing” of  $i_{pmt}$  may dramatically affect the results.

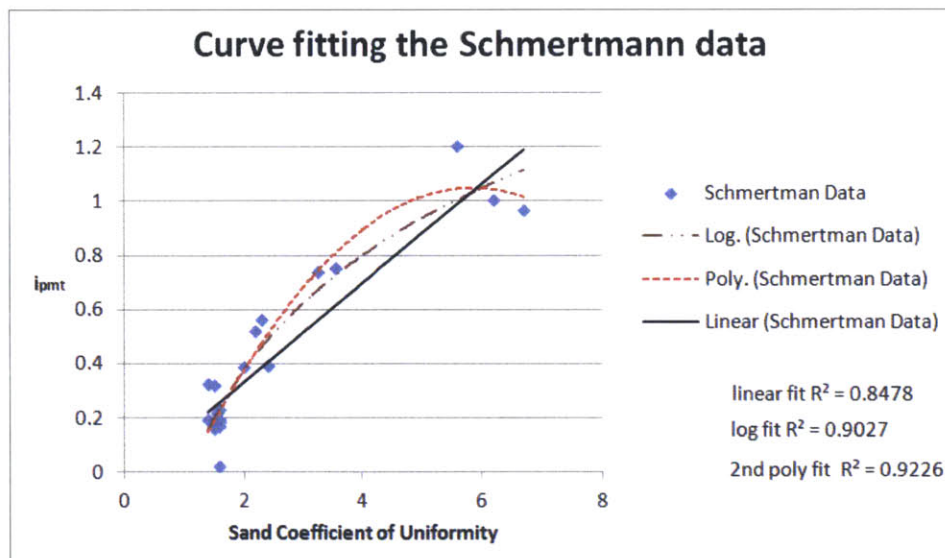


Figure 3.6 Adjustment to the Schmertmann Correlation for Determining  $i_{pmt}$  After Schmertmann, 2000

The Schmertmann methodology was developed to provide a simplified process for determining the critical gradient that causes piping and the factor of safety against piping failure. It is possible that Schmertmann over-simplified the process.

### **3.6 Processing Case Study Data**

The case studies presented in Chapter 4 use field data in the Sellmeijer and Schmertmann methodologies to predict the critical reservoir pool elevation. Two model spreadsheets were created, (one template for the Sellmeijer methodology and one template for the Schmertmann methodology). These spreadsheets are the templates that used to process the actual project data gathered from the two case studies. The input parameters for equation 8, which includes for the individual Sellmeijer scaling factors 8a – 8c (i.e.  $F_R$ ,  $F_S$ ,  $F_G$ ) are shown in the Table 5 and the input parameters are for equation 10, which includes for the individual Schmertmann correction factors 10a – 10h (i.e..  $C_D$ ,  $C_L$ ,  $C_s$ ,  $C_K$ ,  $C_z$ ,  $C_Y$ ,  $C_\alpha$ , and  $C_R$ ) were determined according to Table 6. The spreadsheets are arranged by case study and can be found in Appendix A.

The three key parameters that will be further analyzed to compare the two methodologies are relative density, permeability, and grain size. The results of the two predictive methodologies, Sellmeijer and Schmertmann, are tabulated and, along with the analysis, are presented in Chapter 4.0 for discussion.



## 4.0 Parameters and Data Analysis

Two case studies are presented in this Chapter to demonstrate the use of the Sellmeijer and Schmertmann predictive methodologies for the critical hydraulic gradient of a water impoundment structure (i.e dam). The critical reservoir level (calculated from the gradient) predicted by the two methodologies are compared to determine the most effective use of the methodologies, given the input parameters that define the specific site geology and geometry. The ability to predict critical reservoir pool elevation provides the context for funding dam safety risk reduction measures. With this in mind it is vital to understand the piping mechanism as accurately as possible, starting with the critical hydraulic gradient that produces piping in the dam foundation.

Both the Schmertmann and Sellmeijer methodologies are among the USACE tools in evaluating the predictive behavior of the portfolio dams during the event tree analysis. Understanding the methodology limitations will reduce some of the uncertainty when considering the critical gradient prediction in the estimation of probability for the internal erosion failure mode. The results for the methodologies are central to estimating probability. The Sellmeijer and Schmertmann corrections and scaling factors are applied to the specific geologic input parameters for the two cases, as described in tables 5 and 6, to show the mathematical relationships between flume tests to real project conditions. The Sellmeijer methodology seems to predict a more plausible result on the heterogeneous foundations presented in the two cases; therefore, the Sellmeijer methodology appears to be more applicable when evaluating glacially influenced foundations (i.e. similar to the case studies presented in Section 4.1).

The two case histories that were used to examine the methodologies are from the USACE portfolio. Most of the sources cited were “for Official Use Only” documents and therefore, cannot be specifically cited in this thesis. The projects will be referred to as case A and case B, rather than their respective names, and the specific location has been purposefully omitted from the text. The detailed information from the case study project documents has not been altered, but has been simplified for analysis and presentation purposes. For example, the soil parameters have been averaged to one representative value (i.e. homogeneity is assumed for analysis but in reality the foundation media is not homogenous), and the real foundation stratigraphy is not perfectly horizontal as depicted in the schematic cross sections, figures 4.1 and 4.2. Using the simplified parameters should not affect the comparison of the two methodologies since the same parameters will be used for each methodology.

## **4.1 Case Studies**

This thesis explores the existing conditions at two dam projects located in the northeast and central states of the US. The two dams are large earthen structures and were chosen as simple representations of the USACE portfolio. Data sets were created for each existing case and the data set was used to evaluate the Sellmeijer and Schmertmann methodologies.

Figure 4.1 illustrates the geologic profile, with the minor geologic details, of the Case A dam. The remainder of the site specific parameters that are used in the analysis are located in Appendix A and B for reference.

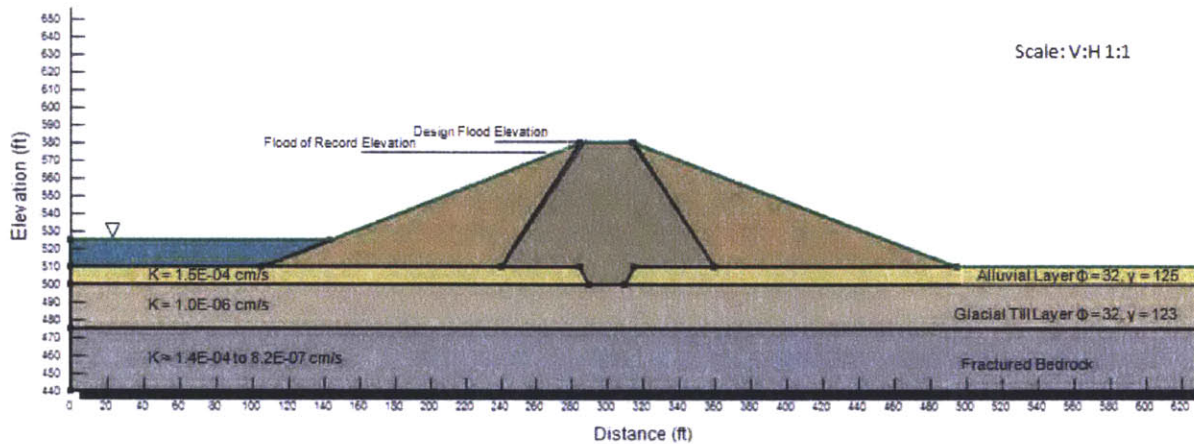


Figure 4.1 Case A Dam Cross Section with Foundation Soil Characteristics Included

Case A is located in the northeast United States within the Worcester Plateau. The topography within the plateau consists of moderately steep hills and mountains with a general North-South trend. Topographic relief within the Worcester Plateau ranges from approximately 400 to 1100 feet above mean sea level (MSL). Little is known about the geomorphology in this area before the Pleistocene era. The only conclusive evidence in this plateau during the Pleistocene era is the Wisconsin glacial advance, which is the last of the four glacial advances. The material deposited directly by the ice is till, and the material deposited by the glacial ice melt water forms the Ice contact features: moraines, eskers, deltas, kettles, kames, and drumlins. The majority of the plateau is covered by ablation till. In stream valleys, alluvium is found in low lying areas subjected to frequent flooding and consisting of gravel sand silt and clay. These deposits consist chiefly of reworked glacial and glaciofluvial materials ranging in size from boulders to silts. The bedrock predominantly consists of metamorphic gneiss, schists, and granofels, deposited to form a discontinuous mantle over igneous and metamorphic rocks in the area.

As shown in Figure 4.1, Case A is a simple 800 foot long earthen dam structure with a small spillway located to the side of the dam. The foundation geology is a shallow layer of both alluvium and glacial outwash built upon weathered bedrock. The topography at the dam site

presents a moderate relief of approximately 300 feet. Both ablation till and basal till can be found at the dam site consisting of dense, poorly sorted mixture of clay, silt sand, gravel, cobbles and boulders deposits (i.e. basal till), as well as deposits that exhibit some degree of stratification, with visible bedding and sorting in the foundation geology (i.e. ablation till). For erosion to be able to progress back to the reservoir, soils overlying the erosion pipe must be able to support a roof along the entire length of the pipe. The embankment material is well compacted SC-SM material that is capable of holding a roof. The dam was built in the 1960s.

Figure 4.2 illustrates the geologic profile, with the minor geologic details, of the Case B dam. The remainder of the site specific parameters that are used in the analysis are located in Appendix C and D for reference.

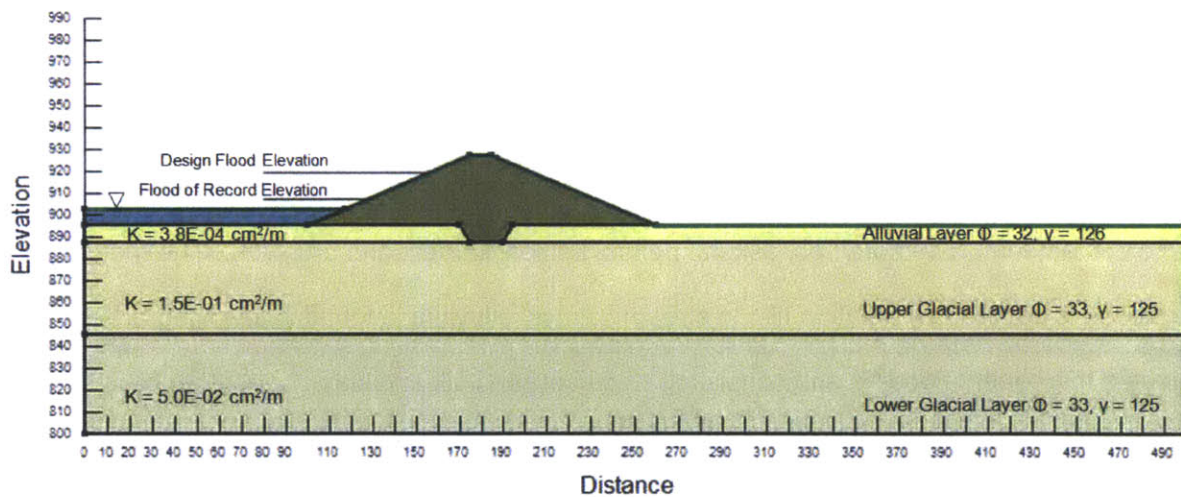


Figure 4.2 Case B Dam Cross Section with Foundation Soil Characteristics Included

Case B is located in the East Central States within the Appalachian Plateau. The topography within the plateau consists of moderately steep to steep hills and mountains with ridges generally aligned in the northeast to southwest direction. Topographic relief within the Appalachian Plateau ranges from approximately 1000 to 3000 feet above mean sea level



(MSL). The upper bedrock units within the plateau were deposited during the Pennsylvanian and Mississippian Periods and consist of alternating layers of sandstones, shales, siltstones, claystones, limestones, and coal often in a cyclic pattern. The bedrock in the vicinity of the dam site is from the Pottsville and Allegheny Formations deposited during the Pennsylvanian geologic period. The dam site has not been covered by glaciers, but glacial ice advanced to the immediate north of the project area has strongly influenced the geology. Landform characteristics of the area have been produced primarily through deposition and erosion cycle of running water. The terrain is generally rugged and hilly, with flat areas primarily occurring within floodplains and on flat-topped terrace features produced by glacial outwash deposition. Outwash and lake deposits occurred in the floodplains and other low lying areas that existed below the glacial margin; these deposits generally consist of gradational layers of clay, silt, sand and gravel.

As shown in Figure 4.2, Case B, is a simple 2500 foot long earthen dam structure with no spillway. The foundation is a shallow layer of alluvium on a deep layer of glacial outwash. The outwash can be divided into an upper and lower zone. The Upper Glacial Outwash is especially pervious and highly variable, generally composed of sands and gravels with only a small amount of silty fine-grained material. The Lower Glacial Outwash is not quite as conductive, and also tends to contain fairly prevalent clay and silt seams. The dam is located in an area that is believed to be the location of a collision between two continental plates. The collision produced a mountain range that eventually eroded away to a rolling topography. This area was later overcome with sediments during the Paleozoic era and then further eroded and sediments were deposited from glacial activity in the area. Alluvium and glacial outwash now cover much of the low lying areas in the floodplain. Crustal movements during the Cretaceous time led to an uplift of the area that forms the Appalachian Plateau. Subsequent movements during the

Tertiary period rejuvenated the streams and a new cycle of erosion began making the hills and valleys more pronounced. The dam site is located in an outwash valley associated with the Illinois and Wisconsin aged glaciations. The dam was built in the 1930s.

The minor geologic details of each case study are presented in section 4.2.

## 4.2 Input Parameters

Each methodology consists of several equations with numerous input parameters. To predict the real conditions one finds, at a dam site, the correction factors need to be applied to scale the parameters according to the analysis of the laboratory tests. The input parameters for case A and case B were defined in Tables 3 and 4, and the method for obtaining the parameter values is described in tables 5 and 6. Table 5 displays the input parameters for the Sellmeijer methodology.

Table 5 Method for Obtaining the Sellmeijer Methodology Inputs

<b>Input Parameter</b>	<b>Method for Obtaining Input Parameter</b>
L	The length of enforced percolation under the dam is obtained from the case cross section.
D	The depth of the soil layer sensitive to piping is obtained from the case cross section.
$\gamma_p$	The unit weight of the soil layer is obtained from the lab test results of the site soil samples.
$\gamma_w$	The unit weight of water is obtained from the lab test results of the site soil samples.
	The angle of internal friction of the soil obtained from the soil samples are used to represent the bedding angle.
k	The permeability is a measure of the soil layer's ability to transmit water through the pore spaces, and is obtained from the field test results.
$\kappa$	The intrinsic permeability is the permeability that is associated with Darcy's law. It is calculated from the soil permeability (k), the viscosity of water ( $\mu = 1.003e-6$ ), and the gravity constant (g). $\kappa = k(\mu/g)$
$\eta$	White's constant is 0.25, which was taken from Sellmeijer's assumption.

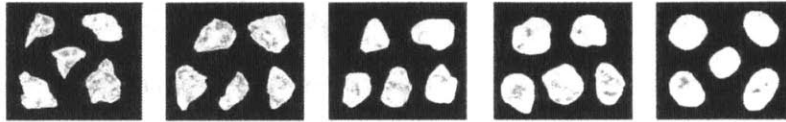
$d_{70}$	The representative grain is obtained from the lab test results of the site soil samples.
RD	The relative density is a correlation of the Standard Proctor Test (SPT) data and the relative density of the soil.
U	The Uniformity coefficient (normally labeled $C_u$ ) is calculated from $d_{60}$ and $d_{10}$ , which are obtained from the lab test results of the site soil samples. $U = d_{60} / d_{10}$
KAS	<p>The soil samples are not available for visible inspection to determine the angularity (i.e. roundness) of the soil particles, so the assumed value for glacial material is 50.</p>  <p>From: (Van Beek, 2010)</p>

Table 6 displays the input parameters for the Schmertmann methodology.

Table 6 Method for Obtaining the Schmertmann Methodology Inputs

Input Parameter	Method for Obtaining Input Parameter
D	Is measured from the cross section.
$L_f$	Is calculated $L / (k_h/k_v)^{0.5}$ , where L is measured from the x-section and $k_h$ and $k_v$ are obtained from the soil testing lab results.
$L_t$	is a measurement of the pipe that formed in the flume test (i.e. 5 ft')
$d_{10f}$	is measurement is made in the lab through sieve analysis and the input value is obtained from the lab test results.
$R_{rk}$	is the ratio of $k_h/k_v$ where $k_h$ and $k_v$ are obtained from the soil testing lab results.
$-D_{rf}$	is the relative density of the soil in the field and an indication of the porosity of the soil. It is determined from a correlation between field standard Proctor test (SPT) data and relative density.
$i_{po}$	Is calculated by applying all the correction factors except $C_a$ to $i_{pmt}$
$i_\alpha$	Is obtained from the Schmertmann interpolation graph located in Appendix G.
R	This is determined from a field measurement. $C_R = 1$ if there is no radius of curvature in the dam.
$R_1$	This is determined from a field measurement. $C_R = 1$ if there is no radius of curvature in the dam.
$R_0$	This is determined from a field measurement. $C_R = 1$ if there is no radius of curvature in the dam.

It is difficult to recreate the dynamics of the seepage and piping behavior in the lab. The lab experiments are idealized conditions that are not often found in the field. For example, the Sellmeijer methodology had a sand test data range  $1.4 < U < 3.5$  (Sellmeijer uses the term  $U$  for uniformity of coefficient), and the Schmertmann methodology had a sand test data range of from  $1.4 < C_u < 6.7$ . Both Case A and Case B are outside the ideal range of testing and validation for both methodologies. The alluvial soil of Case A has a  $C_u = 17$ , which was calculated from the grain size analysis test results of the samples taken from the dam site. The alluvial soil of Case B has a  $C_u = 36.67$ , obtained from sample data of the dam site.

The limited range of use of the two methodologies is disconcerting as the existing field conditions in the USACE portfolio have higher  $C_u$  values, which may make the projects out of the usable range for the methodologies. This means the methodologies can be used as a useful guide, but should not be considered as a true predictive methodology. Therefore, a large uncertainty still exists with regard to predicting the critical gradient of the internal erosion processes at dam sites.

The key input to the Schmertmann methodology,  $i_{pmt}$ , dependent on the  $C_u$  (i.e.  $i_{pmt}$  is obtained through the look up graph of Figure 3.5, which is the correlated critical gradient found in the tests in UF flume relative to the  $C_u$  of the test sand). As explained in Section 3.6.1, the over reliance on the graph makes it difficult to use the Schmertmann methodology for any case that does not have the same starting parameter of  $C_u$ . In an effort to continue with the comparison of the two methodologies, Figure 3.6 was used to generate results that are evaluated. Figure 3.6 estimates a best fit curve for the  $i_{pmt}$  correlation data in the Schmertmann methodology, and assumes an  $i_{pmt}$  value of 1 for any  $C_u$  value over 6. Intuitively, it is noticeable that the values for

the critical gradient in Figure 3.5, and by extension, the critical pool elevations were extremely high and, therefore, unreliable as a predictive methodology for  $C_u$  values outside the range of calibration. The paper written by Schmertmann (2000) suggests that one should not use the Schmertmann methodology for conditions with a  $C_u$  greater than 6, and this author agrees with this.

The Sellmeijer methodology, in contrast to the Schmertmann methodology, was easy to use even though the case studies have a  $C_u$  value outside the range of calibration. The several papers written by Van Beek et al. (2008, 2009, 2010) suggest that the Sellmeijer methodology is only calibrated for fine sands with a  $C_u$  value lower than 3.2 because there were difficulties achieving reliable and repeatable results for coarse grain sands. With the calibration disclaimer in mind, the results from the two cases studies look like reasonable predictive values.

Van Beek et al. (2010) determined through analysis that the uniformity coefficient ( $U$ ) does not affect the Sellmeijer theoretical model output for the range of  $U$  values tested. This means the methodology will function correctly (i.e. one gets reasonable results), but the general applicability of the result is questionable since the equations have not been verified for values outside the range of  $1.4 < U < 3.5$ . Van Beek (2010) further determined through analysis that the  $RD$ ,  $d_{70}$ , and  $k$  have the greatest effect on the  $i_{cr}$  predictive rule defined by Sellmeijer. Relative density is not an actual physical property, and it is not an absolute value. It is an estimation of a physical process in the lab. Natural density has a very small range, and the lab tests for relative density report a range from 0-100%. Figure 4.3 illustrates the effect of relative density on the two methodologies.

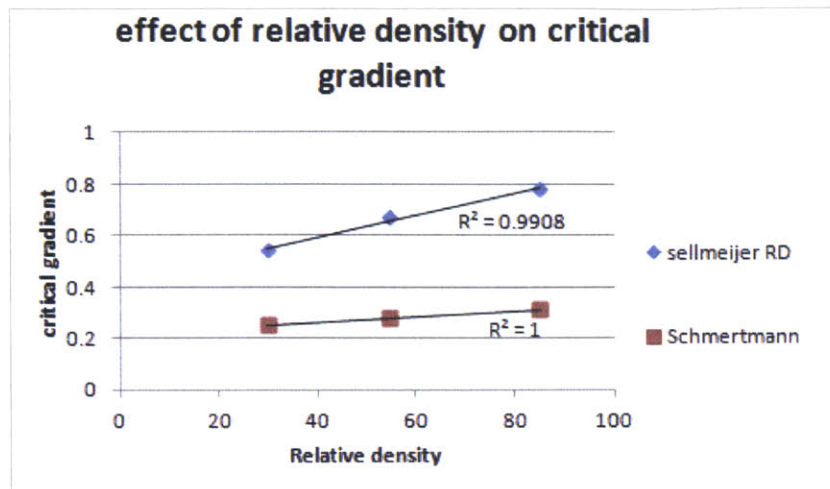


Figure 4.3 Effect of Relative Density on the Sellmeijer and Schmertmann Predictive Methodology

The Schmertmann methodology is not as sensitive to the relative density as the Sellmeijer methodology. Van Beek et al. (Van Beek 2010) were not able to create piping in the test with relative densities less than 50% in the small scale experiments. This means it is possible that less dense foundations may not experience the piping phenomena.

The Sellmeijer and Schmertmann methodologies include the effect of permeability on the critical gradient very differently. Sellmeijer includes the intrinsic permeability of a soil to be consistent with the assumptions of Darcy's Law. Figure 4.4 illustrates the two methodologies with different horizontal axis scales. The graph on the left hand side of Figure 4.4 is a representation of the Sellmeijer scale factor ( $F_s$ ) effect on the critical hydraulic gradient,  $i_{cr}$ , as the permeability is altered; as the permeability of the material increases the water can move more easily through the soil and creates a piping problem, this effect is demonstrated in the glacial layer of the two case studies. Case A glacial till layer has a very low permeability and Case B glacial layer has a relatively high permeability.

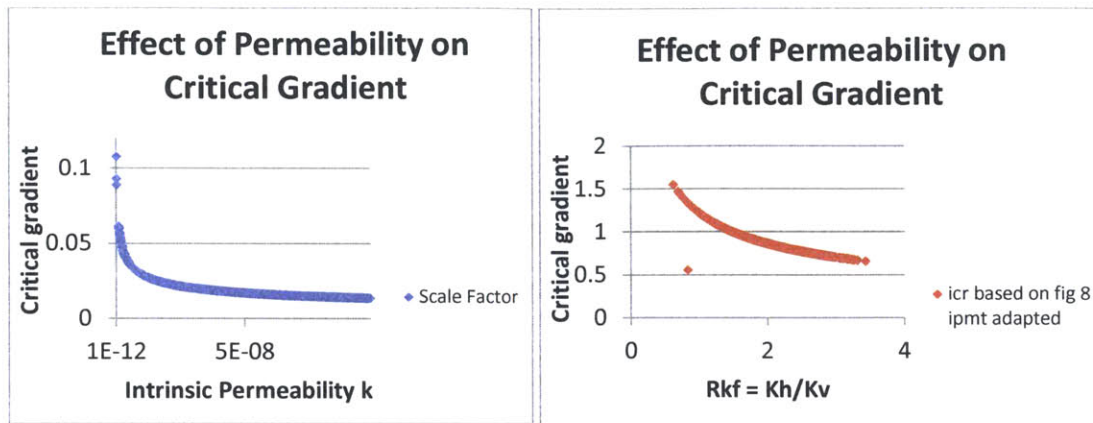


Figure 4.4 Sellmeijer Effect of Intrinsic Permeability (k) and Schmertmann Effect of  $k_h/k_v$

Schmertmann includes the ratio of horizontal permeability to the vertical permeability (i.e.  $R_{fk} = k_v/k_h$ ) to consider the effect that anisotropy of the soil has on the velocity of the groundwater as it flows through the porous foundation. The graph on the right hand side of Figure 4.4 represents the effect that anisotropy has on the Schmertmann methodology. The increase in the  $R_{fk}$  value means there is an increase in the anisotropic soil conditions, and the graph illustrates the effect the  $R_{fk}$  value has on the critical gradient. The critical hydraulic gradient decreases with increased anisotropy due to the increase of seepage velocity, which is a rate dependent variable. Anisotropic conditions concentrate the water into a smaller pipes, thus reducing the cross sectional area, increasing the seepage velocity, and creating a greater piping problem.

There is a significant difference in the way Sellmeijer and Schmertmann approach the interpretation of grain size in their equations. Both methodologies are highly sensitive to an adjustment of grain size as illustrated in Figure 4.5.

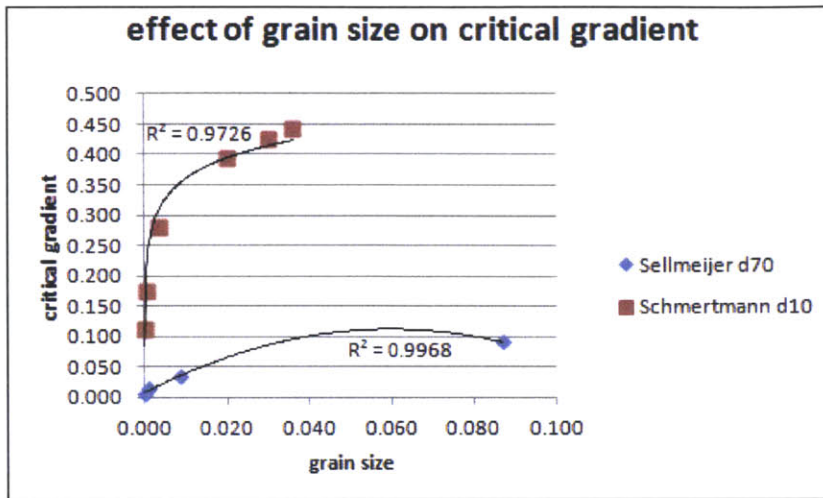


Figure 4.5 Effect of Grain Size (both  $d_{10}$  and  $d_{70}$ ) on the Critical Hydraulic Gradient

Sellmeijer uses the larger sized particles,  $d_{70}$ , in order to analyze the physical process of the particles as they interact with one another, accounting for the frictional resistance in the equilibrium of forces. The use of  $d_{10}$  as the representation of grain size is a common engineering practice and is consistent with Schmertmann's approach. Schmertmann uses the smaller sized particles,  $d_{10}$ , to represent the effect of grain size on the critical gradient calculation because it is a factor in the how easily water can flow through the soil (i.e. permeability of the soil).

### 4.3 Results and Discussion

The Schmertmann and Sellmeijer methodologies were applied to existing dam site input parameters for each case. The two case studies chosen were simple earthen dams with representative features of the USACE portfolio. Both Case A and Case B are outside the range of testing and validation for both methodologies with a  $C_u$  value greater than 6.7. The Sellmeijer methodology had a  $C_u$  test data range of  $1.4 < C_u < 3.5$ , and the Schmertmann methodology had a  $C_u$  test data range of  $1.4 < C_u < 6.7$ . The methodologies were tested with fine sands and



the case studies, which are representative of a large number of glacially influenced dam sites in the USACE portfolio, have very different soil characteristics consistent with glacial alluvium and till.

#### **4.3.1 Case Study Results with Idealized Soil Conditions**

The ideal soil parameters (i.e. Baskarp sand with a uniformity coefficient ( $C_u$ ) = 1.6) used in the flume tests were input into the Sellmeijer and Schmertmann methodologies, while maintaining the geometry of the two case studies to produce the idealized condition prediction results. The variation of the  $C_u$  did not seem to impact the implementation of the Sellmeijer or Schmertmann methodology; however, the accuracy is unknown. The idealized case results seem plausible since the difference of the calculated critical head elevation between the two methodologies is approximately 15 feet in case A and 7 feet in case B. The calculated critical head (i.e.  $H_{crit}$ ) for each methodology is illustrated in figure 4.6 and 4.7. Figure 4.6 is an illustration of the case A system response to the idealized geologic conditions. The  $H_{crit}$  results calculated by the methodologies are displayed as critical reservoir pool elevations.

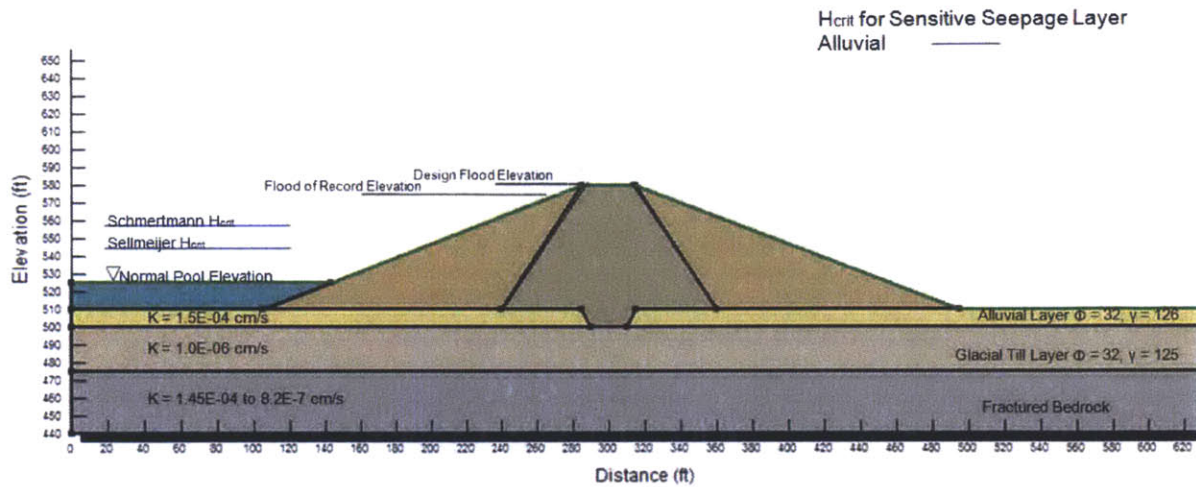


Figure 4.6 Case A – Results of Idealized Predicted Critical Reservoir Elevations for Each Methodology

Figure 4.7 is an illustration of the case B system response to the idealized geologic conditions. The results calculated by the methodologies are displayed as critical reservoir pool elevations ( $H_{crit}$ ).

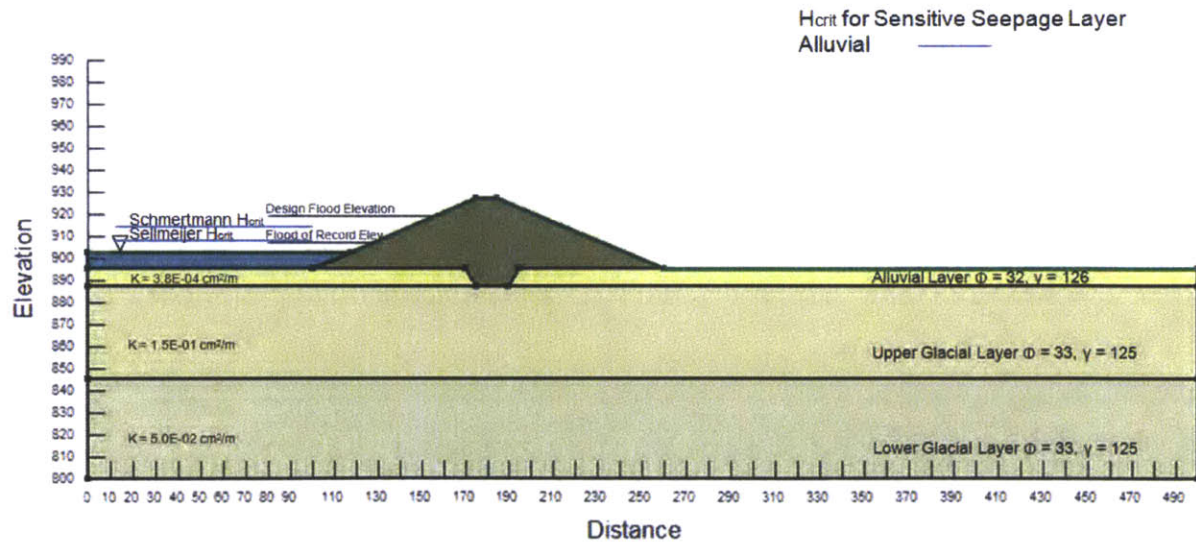


Figure 4.7 Case B – Results of Idealized Predicted Critical Reservoir Elevations for Each Methodology

### 4.3.2 Case A Results

The results for the case A Alluvial Layer were generated from the use of the input parameters and the template spreadsheets located in Appendix A. The resulting critical gradient was calculated and translated to a critical reservoir pool depth to show the expected measurable effect. The results are shown in Table 7 and illustrated in Figure 4.8.

Table 7 Case A Results of the Alluvial Layer

<b>Sellmeijer Results Case A Alluvial Layer</b>					
Icr	Length (ft)	Critical H (m)	Critical H (ft)	Tailwater Elev. (ft)	Critical Reservoir Pool (ft)
0.130	400	15.81	51.34	510.5	561.84
<b>Schmertmann Results Case A Alluvial Layer</b>					
Icr	Length (ft)		Critical H (ft)	Tailwater Elev. (ft)	Critical Reservoir Pool (ft)
0.451	400	-	180.36	510.5	690.86*

\*  $i_{pmt}$  correlation from figure 3.6

The results for the case A Glacial Till layer were generated from the use of the input parameters and the template spreadsheets located in Appendix B. The resulting critical gradient was calculated and translated to a critical reservoir pool depth to show the expected measurable effect. The results are shown in Table 8. The simple analysis of the case studies has assumed that the glacial till layer acts independently of the alluvial layer. It is further assumed for this analysis that the alluvial layer does not exist when the glacial parameters were input into each of the methodologies (i.e. the dam reservoir is in direct contact with the glacial layer since it is assumed that there is no alluvial layer). The results of the glacial layer inputs are illustrated along with the independent alluvial layer results in Figure 4.8.

Table 8 Case A Results for the Glacial Layer

Sellmeijer Results Case A Glacial Till Layer					
icr	L (ft)	Critical H (m)	Critical H (ft)	Tailwater Elev (ft)	Critical Reservoir Pool (ft)
0.671	400	81.78	265.52	510.50	775.97
Schmertmann Results Case A Glacial Till Layer					
icr	Length (ft)		Critical H (ft)	Tailwater Elev (ft)	Critical Reservoir Pool (ft)
0.279	400		111.53	510.50	621.98*

\*  $i_{pmt}$  correlation from figure 3.6

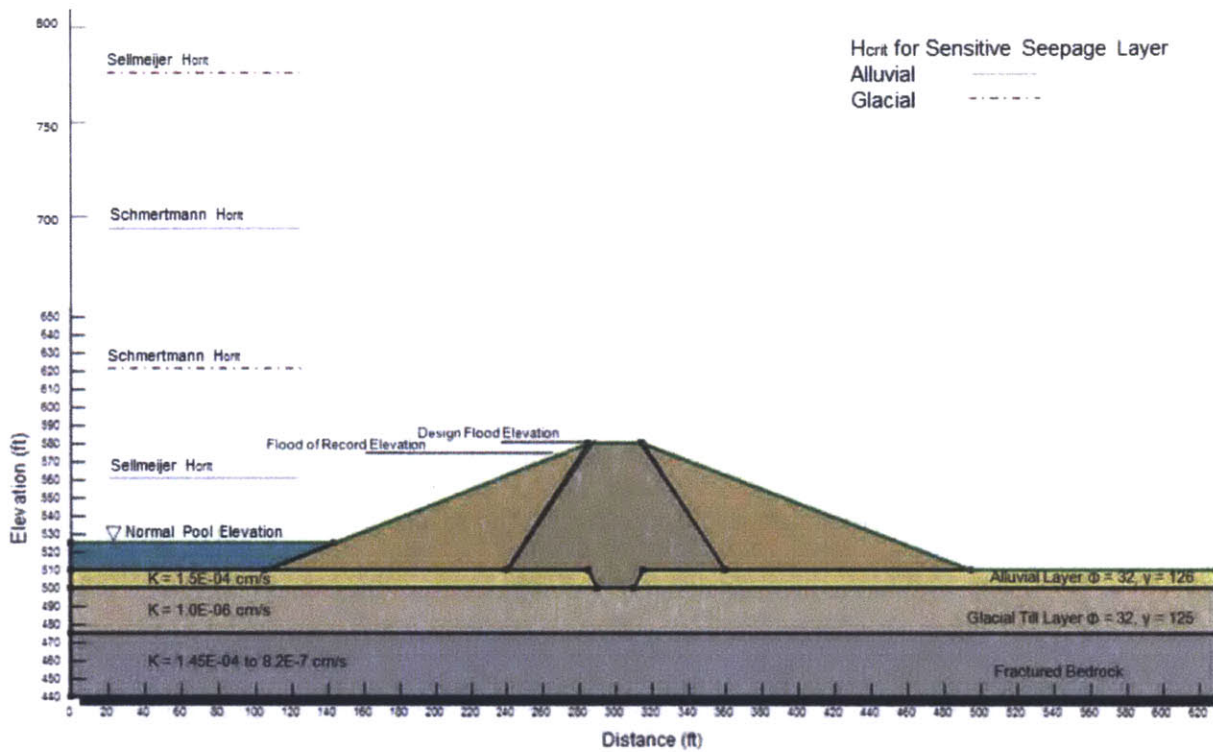


Figure 4.8 Case A – Predicted Critical Reservoir Elevations for Each Methodology

### 4.3.3 Case B Results

The results for the case B Alluvial Layer were generated from the use of the input parameters and the template spreadsheets located in Appendix C. The resulting critical gradient was calculated and translated to a critical reservoir pool depth to show the expected measurable effect. The results are shown in Table 9 and illustrated in Figure 4.9.

Table 9 Case B Results for the Alluvial Layer

<b>Sellmeijer Results Case B Alluvial Layer</b>					
lcr	L (ft)	Critical H (m)	Critical Head (ft)	Tailwater Elev.	Critical Reservoir Pool (ft)
0.052	160	2.56	8.34	895.00	903.34
<b>Schmertmann Results Case B Alluvial Layer</b>					
lcr	Length (ft)		Critical Head (ft)	Tailwater Elev. (ft)	Critical Reservoir Pool (ft)
0.333	160		53.21	895.00	948.21*

\*  $i_{pmt}$  correlation from figure 3.6

The results for the case B Glacial Layer were generated from the use of the input parameters and the template spreadsheets located in Appendix D. The resulting critical gradient was calculated and translated to critical reservoir pool depth to analyze the expected measurable effect. The results are shown in Table 10. The simple analysis of the case studies has assumed that the glacial till layer acts independently of the alluvial layer. It is further assumed for this analysis that the alluvial layer does not exist when the glacial parameters were input into each of the methodologies (i.e. the dam reservoir is in direct contact with the glacial layer since it is assumed that there is no alluvial layer). The results of the glacial layer inputs are illustrated along with the independent alluvial layer results in Figure 4.9.

Table 10 Case B Results for the Glacial Layer

<b>Sellmeijer Results Case B Glacial Layer</b>					
lcr	L (ft)	Critical Head (m)	Critical Head (ft)	Tailwater Elev.	Critical Reservoir Pool
0.029	160	1.41	4.57	895.0	899.57
<b>Schmertmann Results Case B Glacial Layer</b>					
lcr	Length (ft)		Critical Head (ft)	Tailwater Elev. (ft)	Critical Reservoir Pool (ft)
0.385	160		61.65	905.0	966.65*

\*  $i_{pmt}$  correlation from figure 3.6

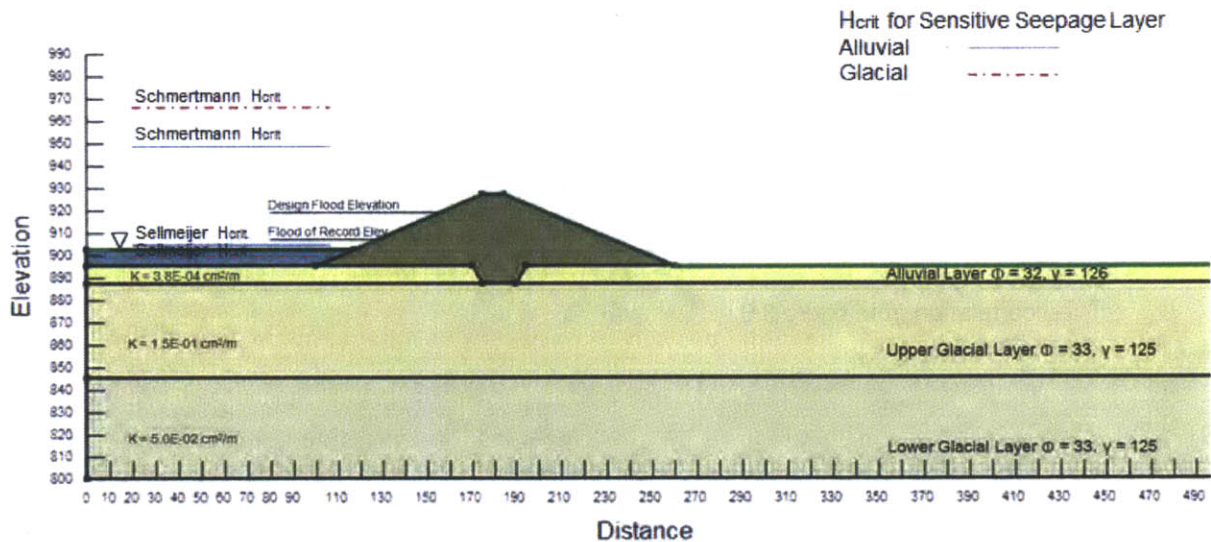


Figure 4.9 Case B – Predicted Critical Reservoir Elevations for Each Methodology

There is a large variation of the critical gradient between the two methodologies, which can be seen in figures 4.8 and 4.9. This is caused by the effect of imposing a fixed  $i_{pmt}$  at a value of 1 for a  $C_u$  value over 6. As described in section 3.5, selecting  $i_{pmt} = 1$  was the best estimate given the circumstances. It is not possible to compare the two methodologies since the key parameter of the Schmertmann methodology,  $i_{pmt}$ , is not accurately obtained at higher  $C_u$  values.

The Sellmeijer methodology has been tested and verified through various experiments and analysis, and it is simple to use. Sellmeijer et al., have been studying the seepage and piping mechanism for the past 20 years. It seems the Sellmeijer methodology is a better predictor than the Schmertmann method due to the fact that the methodology is being continually studied by Sellmeijer et al. and Van Beek et al. The Sellmeijer methodology has evolved and improved

through testing, analysis and further calibration, which has been peer reviewed through the years.

In contrast, independent literature verifying the Schmertmann methodology is scarce. The intention of the Schmertmann methodology was to simplify calculating  $i_{cr}$ . The fact that the methodology relies on three look up graphs that must be performed manually and introduces more subjectivity into the calculation, makes the author of this thesis question the simplicity of the Schmertmann methodology. Furthermore, the explanation on the derivation of the Schmertmann interpolation graphs and the scaling factors is limited. Without the full expression of the derivation it is not possible to specifically verify how the parameter inputs are intended to be used. This makes it difficult to provide consistency and repeatability when different technicians use the methodology for the same case study.





## 5.0 Conclusions and Recommendations

As floodplains become more populated and developed, and people are more reliant on the full functionality of the flood risk management infrastructure, it is essential that engineers better understand the internal erosion mechanism of dams. The analysis of the case studies in Chapter 4 highlights the limitation of applicability of the Sellmeijer and Schmertmann predictive methodologies based on the uniformity coefficient of the dam foundation. Understanding the limitations of the two methodologies will enable the engineering community to further refine the methods, and to improve the general knowledge of the internal erosion behavior of our flood risk management infrastructure.

The Sellmeijer and Schmertmann methodologies are used to predict the internal erosion mechanism by identifying interrelated parameters that, when combined, cause retrogressive piping failure. The Sellmeijer methodology has been tested and verified through various experiments and analyses, and it is simple to use. Sellmeijer et al., and Van Beek et al. are researchers who have extensively verified test results, equations, and assumptions in order to calibrate the Sellmeijer methodology. The methodology has evolved over time with the addition of variables and correction factors. The Sellmeijer methodology is not calibrated for soils with a  $C_u$  over 3.5, but the equations of the methodology still perform as intended on foundations with higher  $C_u$  values. The Schmertmann methodology is over-reliant on the  $i_{pmt}$  variable, which has a strong correlation to the uniformity coefficient of the piping layer. The overreliance renders the methodology inoperative at higher  $C_u$  values. Therefore, it is the recommendation of this author that the Sellmeijer methodology be used as a predictive tool when analyzing the critical gradient of a dam, with the caveat that the results may not be exact.

The Sellmeijer methodology includes the factors to account for scale ( $F_S$ ) and geometry ( $F_G$ ) in the critical gradient calculations to predict the critical reservoir pool of a dam. The Sellmeijer methodology goes one step further and considers the micro interactions of the soil particles and the groundwater as they move through the medium including the resistance factor ( $F_R$ ) in the critical gradient calculations to account for the frictional forces at the micro particle level. The Sellmeijer  $H_{crit}$  results seem plausible for both case studies given the soil parameters.

As found in the case study results, the Schmertmann critical head value is 40' above the dam profile, as calculated using Figure 3.6 for the Alluvial Layer (Figure 4.8). If the correlation that Schmertmann developed in Figure 3.5 was used in the calculation, then the predicted critical head would be even higher. The prediction of the critical head being so high indicates that the dam will never have an internal erosion problem because the dam would overtop well before it had internal erosion issues. This prediction seems unlikely since both the case studies presented have evidence of excessive piping by the presence of sand boils. The Schmertmann interpolative graphs force relationships that fit the conditions in the flume, but the relationships do not seem to fit the two case studies (i.e. real field conditions).

The Baskarp sand parameters (i.e. one of the test soils in the flume tests,  $C_u = 1.6$ , which is within the calibration range of both methodologies) were input into both the Sellmeijer and Schmertmann methodologies to predict the critical hydraulic gradient. The critical reservoir pool depth was within the dam profile height (i.e. not higher than the dam crest) for both methodologies in both cases. Both methodologies produced results that were plausible, demonstrating the value of these predictive methodologies. However, the accuracy of both methodologies is unknown for the higher  $C_u$  values. There are numerous variable parameters

describing the physical geotechnical characteristic of the foundation soils and the assumptions about micro-interactions of soil and water transported through the pore spaces built into the methodologies for determining the critical gradient. Flownets are a useful tool for identifying boundary conditions and visualizing the potential flow of groundwater. However, flownets are a limited tool due to the presumption of equipotential laminar flow through the media. Field conditions throughout the North East and Central US are seldom uniform due to the glacial influence (i.e. high  $C_u$  with a gradation ranging from silt to gravel to cobbles) as seen in the two case studies presented in this paper. The glacial material can have a complex geology that is layered and varies in the range of consolidation and compaction, and can vary in porosity, which is loose (i.e. high permeability material) or tightly packed (i.e. low permeability material). The use of the Sellmeijer and Schmertmann methodologies may be limited since the existing field conditions in the USACE portfolio appear to be out of the calibrated range of the equations. This means the methodology can be used as a useful guide, but should not be considered as a true predictive methodology.

## **5.1 Recommendations for Using Sellmeijer and Schmertmann Methodologies**

The two methodologies (Sellmeijer and Schmertmann) presented in this study should be used prudently as screening tools for predicting the relative critical gradient in dams that have a uniformity coefficient ( $C_u$ ) higher than the tested range. Clearly both processes are designed for use in uniform sands. Both are only tested and calibrated for fine sands at low uniformity ( $C_u$ ) values, although the Schmertmann equation is far more dependent on the soil uniformity than the Sellmeijer equation. There is a large number of existing dams in the USACE portfolio that have less uniform soil characteristics. Although the Sellmeijer methodology is not calibrated for less uniform foundations, the equation seems to give a reasonable estimate of the critical

gradient. The Sellmeijer predictive methodology should be used as the primary critical gradient predictive tool for all dams in the inventory.

The Schmertmann methodology may have a custom application in predicting erosion behavior for dams that have a low uniformity coefficient ( $C_u$ ) and for soils with high  $k_h/k_v$  ratios. Equation 10 has specific correction factors for anisotropic permeability, which is not conspicuously dealt with in the Sellmeijer methodology. Although the Schmertmann methodology incorporates a correction factor to account for varying permeability in anisotropic conditions, the questionable use of the Figure 3.5 in the Schmertmann methodology leads the author to suggest that the Schmertmann methodology not be used as the only method for predicting critical hydraulic gradient. This methodology should be consulted in conjunction with the Sellmeijer methodology and/or modeling software to get complete information on potential piping behavior.

The use of an accurate predictive methodology for determining the critical gradient and critical reservoir pool depth for which internal erosion will lead to dam failure is a beneficial tool in risk management. However, using a model that is not calibrated brings a level of uncertainty into the predicted values. Is there a danger in using a methodology and believing that one has minimized uncertainty in the results of probability of failure? The answer is no if it is used as a screening step and not an absolute prediction of internal erosion. It must be clear to all parties that the methodology is not certain or 100% accurate and further testing is needed to calibrate a reliable predictive tool. Also, site specific hydrogeologic analysis should be required where these methodologies cannot be applied with confidence.

## 5.2 Recommendations for Future Study

It is difficult to model the expected behavior of seepage and erosion because there are many interrelated variables and assumptions required to definitively predict the trigger mechanism for piping. The Sellmeijer and Schmertmann predictive methodologies may not be calibrated to all soil conditions; however, understanding the methodology and potential limitations will enable the subject matter experts to balance the methodology limitations with the prediction results to lower the uncertainty in probability estimates.

Both methodologies are extremely limited to the effective range of  $C_u$  that the equations have been calibrated for in the experimental tests. Additional tests should be performed on more complex soil samples, such as glacial tills and alluvium with anisotropic conditions and that have higher  $C_u$  values. After enough tests are run the methodologies should then be further calibrated for the additional geologic conditions and possible refinements can be made to components of the Sellmeijer and Schmertmann methodologies. Recreating the flume test and using alluvium and glacial till with a broader range of  $C_u$  values should be performed to make more accurate correlations and to calibrate the methodologies for soils with higher  $C_u$  values. The dependency of the Schmertmann methodology on the use of Figure 3.5 suggests that the Schmertmann method only be used for analysis when the soil characteristics fall within the range that the methodology was designed for;  $1.4 < C_u < 6.7$ .

Van Beek (2012) has started to analyze the effect of multi-layered foundations on the Sellmeijer methodology. This should be further explored to account for the potential influence anisotropic conditions may impose on the critical hydraulic gradient. Understanding the heterogeneous

behavior of soil found in the case studies is the key to understanding the piping mechanism better.

Work should be done to connect the existing sources of information available at the dam sites to make a meaningful, site specific, predictive tool. Combining modeling software, real time piezometer data, and Sellmeijer's prediction methodology on the specific site geology, in an interactive database, may help engineers understand the inner soil dynamics of dam foundations better.

It is essential that agencies and organizations with large portfolios of dams understand the tools that they are using to screen and compare projects. If the probability of failure of a project is inaccurately inflated or deflated due to uncertainty during the potential failure mode analysis, then the project position relative to other projects in the priority funding queue may not be correct. This could potentially mean a low risk project may be ranked higher than a high risk project. Understanding the range of applicability of one's risk management tools will enhance one's ability to control and recover from floods, thus saving lives, money, and professional reputation.

## References

1. Abdoun, T., Bennett, V., Dobry, R., Koelewijn, A., Thevanayagam, S. (2010). Real-time monitoring of full-scale levee testing. *Physical modeling in Geotechnics*. ISBN 978-0-415-59288-8, pages 1171 - 1176.
2. AIRMIC, Alarm, IRM, (2010). *A structured approach to Enterprise Risk Management (ERM) and the requirements of ISO 31000*. London, England: UK – The Association of Insurance and Risk Managers (AIRMIC), ALARM The National Forum for Risk Management in the Public Sector, and Institute of Risk Management (IRM).
3. Army Technical Manual No. 5-698-4, (2006). Failure Modes, Effects, and Criticality Analyses (FMECA) For Command, Control, Communications, Computer, Intelligence, Surveillance, and Reconnaissance (C4ISR) Facilities.
4. ASCE (2009). Guiding Principles for the Nations Critical Infrastructure. American Society of Civil Engineers:
5. ASCE (2013). 2013 Report Card for America's Infrastructure. American Society of Civil Engineers: pages 1-74.
6. Bligh, W.G. (1910). Dams, Barrages and Weirs on Porous Foundations. *Engineering News*. Vol 64 No 26, 708-710.
7. Casagrande, A., (1984). Evaluating Calculated Risk in Geotechnical Engineering. *ASCE Journal of Geotechnical Engineering*. Vol. 110, No. 2, pages 314-357.
8. De Wit, J.M., Sellmeijer, J.B., Penning, A. (1981). Laboratory Testing on Piping. Pages 517-520.
9. Einstein, H. (2003). Uncertainty in Rock Mechanics and Rock Engineering - Then and Now. *South African Institute of Mining and Metallurgy. ISRM 2003*, pages 281-293.
10. Freeze, R., and Cherry, A. 1979. *Groundwater*. Prentice-Hall Inc. Englewood Cliffs, N.J. 604p.
11. HSE (2001), U.K. Health and Safety Executive. REDUCING RISKS, PROTECTING PEOPLE, HSE's Decision Making Process. *Her Majesties Stationary Office*. ISBN 0 7176 2151 0, 1-88.
12. Kinnicutt, P., Einstein, H. (1996). Incorporating Uncertainty, Objective, and Subjective Data in Geologic Site Characterization. *ASCE Geotechnical Special Publication*. , pages 104-118.
13. Koenders, M.A., Sellmeijer, J.B. (1992). Mathematical Model for Piping. *Journal of Geotechnical Engineering*. Vol. 118, No. 6, pages 943-946.
14. Lane E. W. (1930). Materials in Existing Earth Dams. *Engineering News Record*. 105, 25, 961-965.
15. Lane E.W. (1934). Security from Under-Seepage Masonry Dams on Earth Foundations. *American Society of Civil Engineers. 1934 Proceedings, Paper 1919*, 1235 -1272.
16. Lane E.W. (1934). Uplift and Seepage Under Dams on Sand. *American Society of Civil Engineers. 1934 Proceedings, Paper 1920*, 1352 -1385.

17. Sellmeijer, J. B. (1988). On the Mechanisms of Piping under Impervious Structures. *PhD thesis*.
18. Sellmeijer, J.B., Koenders, M.A. (1991). A mathematical model for piping. *Appl. Math. Modelling. Vol. 15, Nov/Dec*, pages 646 - 651
19. Sellmeijer, J.B., Weijers, J.B.A. (1993). A new model to deal with the piping mechanism. *Filters in Geotechnical and Hydraulic Engineering. ISBN 90 5410342 6*, pages 349-376.
20. Sellmeijer, J.B. (2006). Numerical computations of seepage erosion below dams (piping); pages 1 -6.
21. Sellmeijer, H., Lopez de la Cruz, J. Van Beek, V., Knoeff, H. (2011). fine tuning of the backward erosion piping model through small-scale, medium-scale and IJkdijk experiments. *EJECE-15/2011. Erosion in geomaterials .* , pages 1139-1154.
22. Terzaghi, K (1929). Effect of Minor Geological Details on the Safety of Dams. *Technical publications of the American Institute of Mining and Metallurgical Engineers. 215*, 31-33
23. Terzaghi, K (1939). Soil Mechanics - A New Chapter in Engineering Science. *Minutes of Proceedings of the James Forrest Lecture. May*, 105-142.
24. Terzaghi, K., Peck, R., Mesri, G., (1996). *Soil Mechanics in Engineering Practices, 3rd edition*. New York: John Wiley & Sons, Inc..
25. USACE ( ), Munger, D., Bowles, D., Boyer, D., Davis, D., Margo, D., Moser, D., Regan, P., Snorteland, N., Interim Tolerable Risk Guidelines for US Army Corps of Engineers Dams. . , 1-17.
26. USACE (2011), Munger, D., Bowles, D., Davis, D., Harper, B., Moser, D. (2011). Levee Safety and Tolerable Risk - Implications For Shared Risk, Responsibility, And Accountability. *31st Annual USSD Conference. ISBN 978-1-884575-52-5*, 1183-1196.
27. USACE (2011). ER 1110-2-1156; Safety of Dams Policy and Procedures. USArmy Corps of Engineers.
28. USACE (2012). Best Management Practices in Dam and Levee Safety Risk Analysis, version 3.
29. Van Beek, V., Koelewijn, A., Kruse, G., Sellmeijer, H., Barends, F. (2008). Laboratory Testing on Piping. *Fourth International Conference on Scour and Erosion. .* , 453-459.
30. Van Beek, V.M., Koelewijn, A.R., Kruse, G.A.M., Sellmeijer, J.B. (2008). Influence of heterogeneities on the formation of piping channels in sand - a first assessment. . , pages 1 - 9.
31. Van Beek, V.M., Koelewijn, A.R., Kruse, G.A.M., Sellmeijer, J.B. (2008). Speculations on the process of piping in laterally heterogeneous sands. *Proceedings of the 19th European Young Geotechnical Engineers' Conference. .* , pages 71-79.
32. Van Beek, V., Knoeff, J.G., de Bruijn, H.T.J., Sellmeijer, J.B. (2009). Influence of sand characteristics on the piping process- Small-scale experiments, 1-10.
33. Van Beek, V., Lujendijk, M.S., Knoeff, J.G., Barends, F.B.J. (2009). Influence of relative density on the piping process- Small-scale experiments, 1-10.
34. Van Beek, V., Knoeff, J.G., Rietdijk, J., Sellmeijer, J.B., Lopez De La Cruz, J. (2010). Influence of sand and scale on the piping process - experiments and multivariate analysis. *Physical Modelling in Geotechnics. ISBN 978-0-415-59288-8*, 1221-1227.



35. Van Beek, V.M., Bezuijen, A., Zwanenburg, C. (2010). Piping: Centrifuge experiments on scaling effects and levee stability. *Physical Modelling in Geotechnics*. ISBN 978-0-415-59288-8, pages 183-187.
36. Van Beek, V.M., de Bruijn, H.T.J., Knoeff, J.G., Bezuijen, A., Forster, U. (2010). Levee Failure Due to Piping: A Full-Scale Experiment. *International Conference on Scour and Erosion 2010. (ICSE-5)*, pages 283-292.
37. Van Beek, V.M., Knoeff, H., Sellmeijer, H. (2011). Observations on the process of backward erosion piping in small, medium, and full scale experiments. *EJECE-15/2011. Erosion in geomaterials.* , pages 1115 - 1137.
38. Van, M.A., Zwanenburg, C., Koelewijn, A.R., van Lottum, H. (2009). Evaluation of Full Scale Levee Stability Tests at Booneschans and Corresponding Centrifuge Tests. *Proceedings of the 17th International Conference on Soil Mechanics and Geotechnical Engineering.* , pages 2048 - 2051.
39. Watson, I., Burnett, A., (1993). *Hydrology, Theory and Application of Ground Water and Surface Water for Engineers and Geologists*. Florida: CRC Press LLC.
40. White, C.M. (1940). The Equilibrium of Grains on the Bed of a Stream. *Proceedings of the Royal Society.* , pages 321-338.

## Websites consulted

1. [Usace.army.mil/missions/civilworks/damsafety](http://Usace.army.mil/missions/civilworks/damsafety)
2. [Infrastructurereportcard.org](http://Infrastructurereportcard.org)
3. [ASCE.org](http://ASCE.org)
4. [USDSO.org](http://USDSO.org)

# **Appendix A**

**Case A**  
Sellmeijer Methodology

Input Parameter	Units	Input Value Alluvial	Input Value Glacial Till
D	m	3.352	7.62
L	m	121.92	121.92
$\gamma_p$	kg/m <sup>3</sup>	20.4	19.6
$\gamma_w$	kg/m <sup>3</sup>	9.8	9.8
$\phi$		32	32
k	m/s	0.0001	0.000001
$\kappa$	m <sup>2</sup>	1.02E-11	1.02E-13
$\eta$	-	0.25	0.25
$d_{70}$	m	0.00077	0.00087
RD	%	41	55
U	%	17	100
KAS	-	70	70

**Case A**  
Schmertmann Methodology

Input Parameter	Units	Input Value Alluvial	Input Value Glacial Till
D	ft	11	25
L	ft	400	400
L <sub>r</sub>	ft	400	400
L <sub>t</sub>	ft	5	5
$d_{10r}$	mm	0.0237	0.0036
k	cm <sup>3</sup> /sec	1.50E-04	1.00E-06
R <sub>k</sub>	-	1	1
D <sub>rr</sub>	%	41	55
ipo	ft	0.488	0.302
i $\alpha$	ft	0.488	0.302
R	ft	-	-
R <sub>1</sub>	ft	-	-
R <sub>0</sub>	ft	-	-

### Case A - Alluvial Layer Sellmeijer Methodology

Resistance Factor - $F_R$				
RDm	Um	KASm	$\Phi$	$F_R = \eta ( \gamma'_r / \gamma_w ) \tan \Phi$
72.5	1.81	49.8	(deg)	
RD	U	KAS	30	0.17
41	17.000	70	31	0.18
$(RD/RD_m)^{0.35}$	$(U/U_m)^{0.13}$	$(KA S/KA S_m)^{-0.02}$	32	0.18
0.82	1.34	0.99		

Scale Factor - $F_S$	
$d_{70}$	0.000770 m
$(d_{70m}/d_{70})^{0.6}$	0.48
$d_{70m}$	L
0.000208	(m)
	$F_S = d_{70} / (kL)^{1/3} (d_{70m}/d_{70})^{0.6}$
	121.92 0.328

Geometrical Factor - $F_G$	
D	3.3528 m
L	$F_G = 0.91(D/L)^{0.28}((0.28(D/L)^{2.8}-1)+.04)$
(m)	
121.92	2.158

Factors		
$F_R$	0.184	Resistance
$F_S$	0.33	Scale
$F_G$	2.158	Geometry
$i_{or}$	0.130	

$\Phi$ (deg)	$i_{or}$	L (ft)	Critical H (m)	Critical H (ft)	Tailwater Elev.	critical Pool
32	0.130	400.0	15.815	51.348	510.500	561.848

### Case A - Alluvial Layer Schmertmann Methodology

$C_D$	
UF Flume Length	5
Example Pipe Length	400
$C_D$	1.468

$C_s$	
avg grain size	0.20
Exponent	0.2
$C_s$	0.653

$C_a$	
$i_{ao}$	0.488
$\alpha$	0
$i_{ao}$ from graph	0.488
$C_a$	1.00

$C_L$	
UF Flume Length	5
Exponent	0.2
$C_L$	0.418

$C_{K1}$	
UF Flume Anisotropy	1.5
Exponent	0.5
$C_{K1}$	1.225

$C_{R1}$	
R	n/a
R0	n/a
R1	n/a
$C_{R1}$	1.00

$C_z$	
from graph if $D/r < 80$ ; else, $C_z \sim 1.0$	
$K_u/K_o$	0.01
representative r =	0.01
D/r	335
$C_z$	1.00

$C_{D1}$	
D/r	41.00
Exponent	0.2
$C_{D1}$	0.924

$i_{pm}$ if $C_u = 5.5$	$i_{pm}$ from graph
1	estimate from fig 3.6
2.978	Schmertmann eq. 19
1.083	$i = (\gamma_{sat} - \gamma_w) / \gamma_w$

Factors		
$C_D$	1.468	(D/L) Factor
$C_L$	0.418	total pipe length Factor
$C_s$	0.653	Force Factor
$C_{K1}$	1.225	Permeability Anisotropy Factor
$C_z$	1	High Permeability Underlayer Factor
$C_v$	0.924	Density Factor
$C_a$	1.00	Pipe Inclination Adjustment Factor
$C_{R1}$	1	Dam Axis Curvature Factor
	0.451	

$i_{or}$	Length (ft)	Critical Head (ft)	Tailwater Elev. (ft)	Critical Pool (ft)
Schmertmann $i_{pm}$ correlation				
0.451	400	180.362	510.500	690.862
Schmertmann $i_{pm}$ equation 19				
1.343	400	537.118	510.500	1,047.618

## **Appendix B**

**Case A**  
Sellmeijer Methodology

Input Parameter	Units	Input Value Alluvial	Input Value Glacial Till
D	m	3.352	7.62
L	m	121.92	121.92
$\gamma_p$	kg/m <sup>3</sup>	20.4	19.6
$\gamma_w$	kg/m <sup>3</sup>	9.8	9.8
$\Phi$		32	32
k	m/s	0.0001	0.000001
$\kappa$	m <sup>2</sup>	1.02E-11	1.02E-13
$\eta$	-	0.25	0.25
d <sub>70</sub>	m	0.00077	0.00087
RD	%	41	55
U	%	17	100
KAS	-	70	70

**Case A**  
Schmertmann Methodology

Input Parameter	Units	Input Value Alluvial	Input Value Glacial Till
D	ft	11	25
L	ft	400	400
L <sub>r</sub>	ft	400	400
L <sub>t</sub>	ft	5	5
d <sub>10r</sub>	mm	0.0237	0.0036
k	cm <sup>3</sup> /sec	1.50E-04	1.00E-06
R <sub>k</sub>	-	1	1
D <sub>rr</sub>	%	41	55
ip <sub>0</sub>	ft	0.488	0.302
i <sub><math>\alpha</math></sub>	ft	0.488	0.302
R	ft	-	-
R <sub>1</sub>	ft	-	-
R <sub>0</sub>	ft	-	-

**Case A - Glacial Till Layer  
Sellmeijer Methodology**

Resistance Factor - $F_R$				
RDm	Um	KA Sm	$\Phi$	
72.5	1.81	49.8	(deg)	
RD	U	KA S	32	0.24
55	100.000	70		
$(RD/RD_m)^{0.25}$	$(U/U_m)^{0.13}$	$(KA/KA Sm)^{-0.02}$	$F_R = \eta (Y'_{r'} / Y_w) \tan \Phi$	
0.91	1.88	0.99	0.24	

Scale Factor - $F_S$		
$d_{70}$	0.000870	m
$(d_{70m}/d_{70})^{0.6}$	0.42	
$d_{70m}$	L	$F_S = d/0 / (\pi L)^{1/3} (d/0m/d/0)^{0.6}$
0.000208	(m)	121.92 1.591

Geometrical Factor - $F_G$	
D	7.52 m
L	$F_G = 0.91 * (D/L)^{0.28} / ((0.28 / (D/L)^{2.8} - 1) + 0.4)$
(m)	
121.92	1.771

Factors		
$F_R$	0.238	Resistance
$F_S$	1.59	Scale
$F_G$	1.771	Geometry
$i_{cr}$	0.671	

$\Phi$ (deg)	$i_{cr}$	L (ft)	Critical H (m)	Critical H (ft)	Tailwater Elev.	crit Pool
32	0.671	400.0	81.782	265.525	510.450	775.975

**Case A - Glacial Till Layer  
Schmertmann Methodology**

$C_D$	
UF Flume Length	5
Example Pipe Length	400
$C_D$	1.248

$C_S$	
avg grain size	0.20
Exponent	0.2
$C_S =$	0.448

$C_a$	
$i_{50}$	0.302
a	0
$i_{50}$ from graph	0.302
$C_a =$	1.00

$C_L$	
UF Flume Length	5
Exponent	0.2
$C_L =$	0.416

$C_K$	
UF Flume Anisotropy	1.5
Exponent	0.5
$C_K =$	1.225

$C_R$	
R	n/a
R0	n/a
R1	n/a
$C_R =$	1.00

Factors		
$C_D$	1.248	(D/L) Factor
$C_L$	0.416	total pipe length Factor
$C_S$	0.448	Force Factor
$C_K$	1.225	Permeability Anisotropy Factor
$C_H$	1	High Permeability Underlayer Factor
$C_Y$	0.980	Density Factor
$C_i$	1.00	Pipe Inclination Adjustment Factor
$C_R$	1	Dam Axis Curvature Factor
	0.279	

$C_Z$	
from graph if $K_u K_D > 1$ and $D/r < 80$	
$K_u K_D$	1.00
representative r =	0.01
D/r	762
$C_Z =$	1.00

$C_Y$	
D/r	55.00
Exponent	0.2
$C_Y =$	0.980

$i_{crit}$ if $C_u < 3.2$	$i_{crit}$ from graph
1	estimate from fig 3.6
18.167	Schmertmann eq. 19
1.083	$i = (y_{ss} - y_w) / y_w$

$i_{cr}$	Length (ft)	Critical Head (ft)	Tailwater Elev (ft)	Critical Pool (ft)
Schmertmann $i_{cr}$ correlation				
0.279	400	111.534	510.450	621.984
Schmertmann $i_{cr}$ equation 19				
5.086	400	2,026.244	510.450	2,536.694

## **Appendix C**



Case B  
Sellmeijer Methodology

Input Parameter	Units	Input Value Alluvial	Input Value Glacial Till
D	m	1.52	10.668
L	m	49.28	49.28
$\gamma_p$	kg/m <sup>3</sup>	19.6	19.6
$\gamma_w$	kg/m <sup>3</sup>	9.8	9.8
$\phi$		32	33
k	m/s	3.80E-04	1.50E-01
$\kappa$	m <sup>2</sup>	3.88E-11	1.53E-08
$\eta$		0.25	0.25
$d_{70}$	m	0.00015	0.0125
RD	%	29	31
U	%	36.67	44.28
KAS		70	70

Case B  
Schmertmann Methodology

Input Parameter	Units	Input Value Alluvial	Input Value Glacial Till
D	ft	7	35
L	ft	160	160
$L_r$	ft	160	113.13
$L_t$	ft	5	5
$d_{10}$	mm	0.003	0.21
k	cm <sup>3</sup> /sec	3.40E-04	1.50E-01
$R_{rk}$	-	1	2
$D_{rr}$	%	32	30
$i_{po}$	ft	0.334	0.387
$i_a$	ft	0.334	0.387
R	ft	-	-
$R_s$	ft	-	-
$R_d$	ft	-	-

### Case B - Alluvial Layer Sellmeijer Methodology

Resistance Factor - $F_R$				
R Dm	U m	K A S m	$\Phi$	$F_R = \eta (\gamma_r / \gamma_w) \tan \Phi$
72.5	1.81	49.8	(deg)	
RD	U	KAS		0.16
30	36.670	70	31	0.16
$(RD/RD_m)^{0.35}$	$(U/U_m)^{0.13}$	$(KA S/KA S_m)^{0.02}$	32	0.17
0.73	1.48	0.99		

Scale Factor - $F_S$		
$d_{r,c}$	0.000150	m
$(d_{r,c}/d_m)^{0.6}$	1.22	
$d_{r,m}$	L	$FS = d_{r0} / (\kappa L)^{1/3} (d_{r0}/d_{r0})^{0.6}$
0.000208	(m)	49.28 0.147

Geometrical Factor - $F_G$	
D	1.52 m
L	$F_G = 0.91 \eta (D/L)^{0.28} ((D/L)^{2.8} - 1)^{0.04}$
(m)	49.28 2.097

Factors		
$F_R$	0.169	Resistance
$F_S$	0.15	Scale
$F_G$	2.097	Geometry
$i_{or}$	0.052	

$i_{or}$	L (ft)	Critical H (m)	Critical H (ft)	Tailwater Elev. crit Pool
0.052	160.0	2.569	8.342	895.000 903.342

### Case B - Alluvial Layer Schmertmann Methodology

$C_D$	
UF Flume Length	5
Example Pipe Length	180
$C_D$	1.430

$C_a$	
avg grain size	0.20
Exponent	0.2
$C_a$	0.432

$C_a$	
$i_{or}$	0.334
a	0
$i_{or}$ from graph	0.334
$C_a$	1.00

$C_L$	
UF Flume Length	5
Exponent	0.2
$C_L$	0.500

$C_k$	
UF Flume Anisotropy	1.5
Exponent	0.5
$C_k$	1.225

$C_R$	
R	n/a
R <sub>0</sub>	n/a
R <sub>1</sub>	n/a
$C_R$	1.00

Factors		
$C_D$	1.430	(DL) Factor
$C_L$	0.500	total pipe length Factor
$C_a$	0.432	Force Factor
$C_k$	1.225	Permeability Anisotropy Factor
$C_R$	1	High Permeability Underlayer Factor
$C_\gamma$	0.880	Density Factor
$C_\alpha$	1.00	Pipe Inclination Adjustment Factor
$C_{i1}$	1	Dam Axis Curvature Factor
	0.333	

$C_\gamma$	
from graph if $D/r < 80$ ; else, $C_\gamma \sim 1.0$	
$K_u K_o$	441.18
representative r =	0.01
D/r	152
$C_\gamma$	1.00

$C_\gamma$	
D/r	30.00
Exponent	0.2
$C_\gamma$	0.880

$i_{or}$ for $C_D = 3.2$	$i_{or}$ from graph
1	estimate from fig 3.8
6.578	Schmertmann eq. 19
1.003	$i = (\gamma_{sat} - \gamma_w) / \gamma_w$

$i_{or}$	Length (ft)	Critical Head (ft)	Tailwater Elev. (ft)	Critical Pool (ft)
Schmertmann $i_{or}$ correlation				
0.333	160	53.215	895.000	948.215
Schmertmann $i_{or}$ equation 19				
2.188	160	350.028	895.000	1,245.028

## **Appendix D**

Case B  
Sellmeijer Methodology

Input Parameter	Units	Input Value Alluvial	Input Value Glacial Till
D	m	1.52	10.668
L	m	49.28	49.28
$\gamma_g$	kg/m <sup>3</sup>	19.6	19.6
$\gamma_w$	kg/m <sup>3</sup>	9.8	9.8
$\phi$		32	33
k	m/s	3.80E-04	1.50E-01
$\kappa$	m <sup>2</sup>	3.88E-11	1.53E-08
$\eta$		0.25	0.25
$d_{10}$	m	0.00015	0.0125
RD	%	29	31
U	%	36.67	44.28
KAS		70	70

Case B  
Schmertmann Methodology

Input Parameter	Units	Input Value Alluvial	Input Value Glacial Till
D	ft	7	35
L	ft	160	160
$L_r$	ft	160	113.13
$L_t$	ft	5	5
$d_{10}$	mm	0.003	0.21
k	cm <sup>3</sup> /sec	3.40E-04	1.50E-01
$R_k$	-	1	2
$D_r$	%	32	30
$i_{po}$	ft	0.334	0.387
$i_a$	ft	0.334	0.387
R	ft	-	-
$R_i$	ft	-	-
$R_d$	ft	-	-

## Case B - Glacial Layer Sellmeijer Methodology

Resistance Factor - $F_R$					
RDm	Um	KA sm	$\phi$	(deg)	
72.5	1.81	49.8	31	0.17	
RD	U	KA s	$\phi$		
32	44.286	70	33	0.18	
$(RD/RD_m)^{0.35} (U/U_m)^{0.13} (KA/KA_{sm})^{-0.02} F_R = \eta (\gamma_w/\gamma_w) \tan \phi$					
0.75	1.52	0.99		0.18	

Scale Factor - $F_S$		
$d_{70}$	0.012500	m
$(d_{70}/d_{70m})^{0.6}$	0.09	
$d_{70m}$	L	$F_S = d70 / (KL)^{1/3} (d70m/d70)^{0.6}$
0.000208	49.28	0.118

Geometrical Factor - $F_G$	
D	10.666 m
L	$F_G = 0.91 \sqrt{(D/L)^2 + (0.28(D/L)^2 - 1)^2} - 0.04$
(m)	
49.28	1.322

Factors		
$F_R$	0.184	Resistance
$F_S$	0.12	Scale
$F_G$	1.322	Geometry
$i_{or}$	0.029	

$i_{or}$	L (ft)	Critical H (m)	Critical H (ft)	Tailwater Elev. or Crit Pool
0.029	160.0	1.410	4.579	895.000 899.579

## Case B - Glacial Layer Schmertmann Methodology

$C_D$	
UF Flume Length	5
Example Pipe Length	180
$C_D$	0.926

$C_S$	
avg grain size	0.20
Exponent	0.2
$C_S$	1.010

$C_a$	
$i_{or}$	0.387
$a$	0
$i_{or}$ from graph	0.387
$C_a$	1.00

Factors		
$C_D$	0.926	(D/L) Factor
$C_L$	0.536	total pipe length Factor
$C_S$	1.010	Force Factor
$C_K$	0.888	Permeability Anisotropy Factor
$C_z$	1	High Permeability Underlayer Factor
$C_v$	0.888	Density Factor
$C_e$	1.00	Pipe Inclination Adjustment Factor
$C_R$	1	Dam Axis Curvature Factor
	0.385	

$C_L$	
UF Flume Length	5
Exponent	0.2
$C_L$	0.536

$C_K$	
UF Flume Anisotropy	1.5
Exponent	0.5
$C_K$	0.888

$C_R$	
R	n/a
R0	n/a
R1	n/a
$C_R$	1.00

$i_{or}$	Length (ft)	Critical Head (ft)	Tailwater Elev. (ft)	Critical Pool (ft)
Schmertmann $i_{or}$ correlation	0.385	160	61.651	905.000 966.651
Schmertmann $i_{or}$ equation 19	3.071	400	1,228.591	510.450 1,738.041

$C_z$	
from graph if $K_u/K_s > 1$ and $D/r < 80$	
$K_u/K_s$	0.33
representative $r$	0.01
$D/r$	1067
$C_z$	1.00

$C_v$	
$D/r$	32.00
Exponent	0.2
$C_v$	0.888

$i_{or}$ if $C_u < 3.2$	$i_{or}$ from graph
1	estimate from fig 3.6
7.971	Schmertmann eq. 19
1.003	$i = (\gamma_{se} - \gamma_w) / \gamma_w$

## Appendix E

## Idealized Alluvial Layer Case A and Case B

Sellmeijer

Input Parameter	Units	Case A Idealized Alluvial Layer	Case B Idealized Alluvial Layer
D	m	3.352	2.133
L	m	121.92	49.28
$\gamma_p$	kg/m <sup>3</sup>	19.6	19.6
$\gamma_w$	kg/m <sup>3</sup>	9.8	9.8
$\phi$		37	37
k	m/s	6.50E-05	6.50E-05
$\kappa$	m <sup>2</sup>	6.63E-12	6.63E-12
$\eta$	-	0.25	0.25
$d_{70}$	m	.000154	.000154
RD	%	71	71
U	%	1.6	1.6
KAS	-	50	50

**Case A - Idealized Alluvial Layer  
Sellmeijer Methodology**

Resistance Factor - $F_R$				
RDm	Um	KASm	$\phi$	$F_R = \eta (y_w / y_w) \tan \phi$
72.5	1.81	48.8	(deg)	
RD	U	KAS	30	0.16
71	1.600	70	31	0.16
$(RD/RD_m)^{0.35}$	$(U/U_m)^{0.13}$	$(KAS/KAS_m)^{0.02}$	37	0.20
0.98	0.98	0.98		

Scale Factor - $F_s$	
$d_{15}$	0.000154 m
$(d_{15}/d_{50})^{0.6}$	1.20
$d_{50}$	0.000208 (m)
L	121.92
FS = $d_{70} / (d_{15})^{1/3} (d_{70}/d_{70})^{0.6}$	0.196

Geometrical Factor - $F_g$	
D	3.3528 m
L	$F_g = 0.91(D/L)^{0.28}(D/L)^{2.6-1} + 0$
(m)	2.156

Factor	Value	Description
$F_R$	0.196	Resistance
$F_s$	0.20	Scale
$F_g$	2.156	Geometry
$f_c$	0.005	

$\phi$ (deg)	$f_c$	L (ft)	Critical H (ft)	Tailwater Elev	Critical Pool
37	0.005	400.0	10.305	33.271	510.500

**Case A - Idealized Alluvial Layer  
Schmertmann Methodology**

$C_0$	
UF Flume Length	5
Example Pipe Length	400
$C_0$	1.480

$C_1$	
avg grain size	0.20
Exponent	0.2
$C_1$	0.858

$C_2$	
$e_s$	0.725
$e$	0
$e_s$ from graph	0.725
$C_2$	1.00

Factor	Value	Description
$C_0$	1.480	(D/L) Factor
$C_1$	0.416	total pipe length Factor
$C_2$	0.858	Force Factor
$C_3$	1.225	Permeability Anisotropy Factor
$C_4$	1	High Permeability Underlayer Factor
$C_5$	1.044	Density Factor
$C_6$	1.00	Pipe Inclination Adjustment Factor
$C_7$	1	Dam Axis Curvature Factor
$C_8$	0.870	

$C_L$	
UF Flume Length	5
Exponent	0.2
$C_L$	0.416

$C_R$	
UF Flume Anisotropy	1.5
Exponent	0.5
$C_R$	1.225

$C_R$	
R	na
R0	na
R1	na
$C_R$	1.00

$f_c$	Length (ft)	Critical Head (ft)	Tailwater Elev (ft)	Critical Pool (ft)
Schmertmann $f_c$ correlation				
0.670	400.0	267.868	510.500	778.368
Schmertmann $f_c$ equation 19				
0.107	400.0	42.806	510.500	563.306

$C_z$	
from graph if $D_e < 80$ , else, $C_z = 1.0$	
$F_u/K_e$	0.01
representative $r =$	0.01
$D_e$	336
$C_z$	1.00

$C_z$	
$D_e$	71.00
Exponent	0.2
$C_z$	1.044

$f_c$ from eq 32	$f_c$ from graph
1	estimate from fig 3.5
0.160	Schmertmann eq 19
1.083	$f = (y_w - y_w) / y_w$



# Appendix F

## Idealized Alluvial Layer Case A and Case B

Sellmeijer

Input Parameter	Units	Case A Idealized Alluvial Layer	Case B Idealized Alluvial Layer
D	m	3.352	2.133
L	m	121.92	49.28
$\gamma_p$	kg/m <sup>3</sup>	19.6	19.6
$\gamma_w$	kg/m <sup>3</sup>	9.8	9.8
$\Phi$		37	37
k	m/s	6.50E-05	6.50E-05
$\kappa$	m <sup>2</sup>	6.63E-12	6.63E-12
$\eta$	-	0.25	0.25
$d_{70}$	m	.000154	.000154
RD	%	71	71
U	%	1.6	1.6
KAS	-	50	50

### Case B - Idealized Alluvial Layer Sellmeijer Methodology

Resistance Factor - $F_R$				
RDm	Um	KA Sm	$\phi$	$F_R = \eta (y_s / y_w) \tan \phi$
72.5	1.81	49.8	(deg)	
RD	U	KA S		
71	1.800	70	30	0.14
			31	0.15
$(RD/RD_m)^{0.35}$	$(U/U_m)^{0.13}$	$(KA S/KA S_m)^{-0.02}$	32	0.16
0.99	0.98	0.99		

Scale Factor - $F_S$		
$d_{75}$	0.000154	m
$(d_{75}/d_{75})^{0.5}$	1.20	
$d_{90}$	L	$F_S = d70 / (dL)1/3 (d70m/d70)^{0.5}$
0.000205	(m)	49.25
		0.268

Geometrical Factor - $F_G$	
D	2.133 m
L	$F_G = 0.91(D/L)^{(0.28(D/L)^{2.5-1}+0.4)}$
(m)	
49.28	1.934

Factors		
$F_R$	0.152	Resistance
$F_S$	0.27	Scale
$F_G$	1.934	Geometry
$K_r$	0.078	

Loc	L (ft)	Critical H (ft)	Tailwater Elev. crit Pool
0.078	160.0	3.880	12.598
			895.000
			907.598

### Case B - Idealized Alluvial Layer Schmertmann Methodology

$C_p$	
UF Rume Length	5
Example Pipe Length	180
$C_p$	1.337

$C_s$	
avg grain size	0.20
Exponent	0.2
$C_s$	0.858

$C_a$	
$\omega$	0.738
$\alpha$	0
$\omega$ from graph	0.738
$C_a$	1.00

Factors		
$C_p$	1.337	(DL) Factor
$C_s$	0.850	total pipe length Factor
$C_a$	0.858	Force Factor
$C_k$	1.225	Permeability Anisotropy Factor
$C_z$	1	High Permeability Underlayer Factor
$C_d$	1.044	Density Factor
$C_i$	1.00	Pipe Inclination Adjustment Factor
$C_c$	1	Dam Axis Curvature Factor
	0.734	

$C_e$	
UF Rume Length	5
Exponent	0.2
$C_e$	0.800

$C_h$	
UF Rume Anisotropy	1.5
Exponent	0.5
$C_h$	1.225

$C_m$	
R	n/a
R0	n/a
R1	n/a
$C_m$	1.00

Loc	Length (ft)	Critical Head (ft)	Tailwater Elev (ft)	Critical Pool (ft)
Schmertmann low correlation				
0.734	160	117.361	895.000	1,012.361
Schmertmann low equation 19				
0.117	180	18.754	895.000	913.754

$C_r$	
form graph if $D/r < 80$ , else, $C_r = 1.0$	
$K_u/K_c$	441.18
representative $r$	0.01
$D/r$	213
$C_r$	1.00

$C_d$	
$D_r$	71.00
Exponent	0.2
$C_d$	1.044

test $D_r < 150$	low from graph
1	estimate from fig 3.6
0.160	Schmertmann eq 19
1.003	$r = (y_w - y_s) / y_w$

# Appendix G

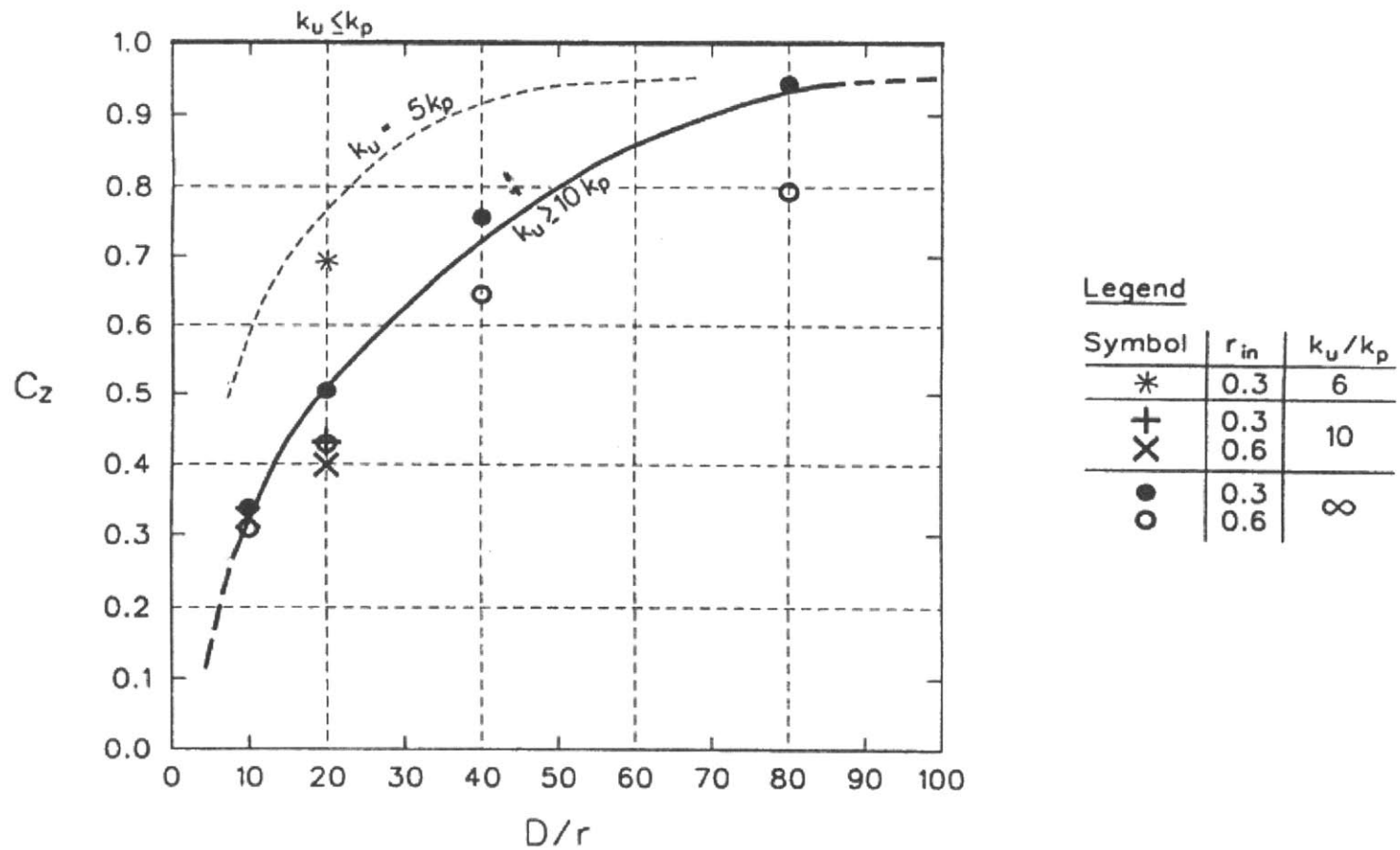


**FIGURE 12** HIGH ( $k_u/k_p$ ) UNDERLAYER CORRECTION -  $C_z$ ,  
 BASED ON COMPARISON OF  $i_{ve}$  FROM COMBINED  
 2-D CROSS- AND LONGITUDINAL-SECTION FLOWNETS  
 OF UF FLUME

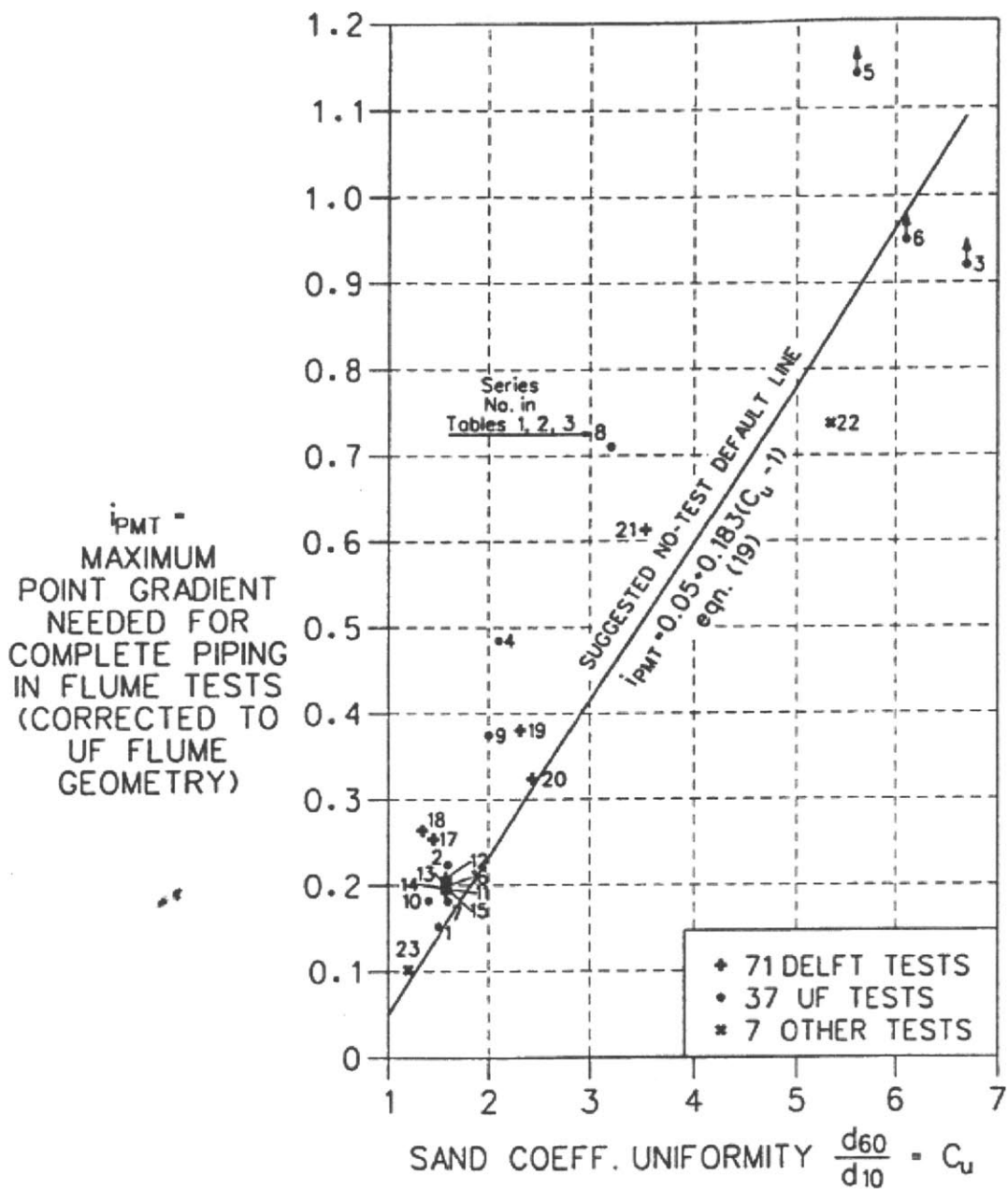


**FIGURE 6**  $C_{DGL}$ -CORRECTED HORIZONTAL PIPING GRADIENTS WITH A NO-TEST DEFAULT LINE (USING UF-TEST REFERENCE  $L=5.0$  FT AND  $D/L=0.20$ )

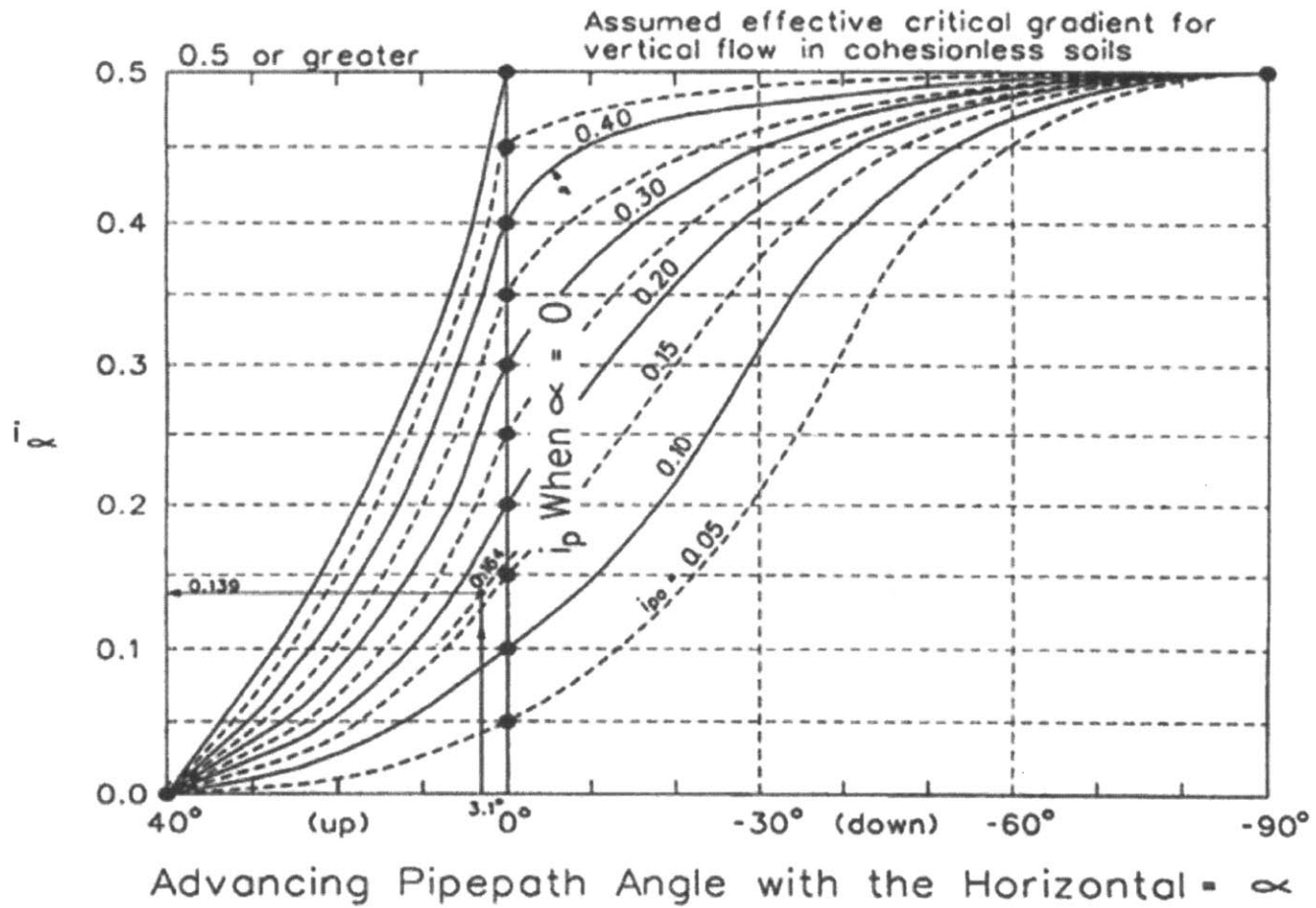


**FIGURE 13** INTERPOLATION GRAPH TO ESTIMATE  $i_p$  FOR NON-HORIZONTAL PIPEPATHS